Gondwana Research 38 (2016) 183–196

Contents lists available at ScienceDirect

Gondwana Research

journal homepage: www.elsevier.com/locate/gr

Paleotethyan evolution of the Indochina Block as deduced from granites in northern Laos

Shifeng Wang [a,*], Yasi Mo [b], Chao Wang [b], Peisheng Ye [a]

[a] Institute of Geomechanics, Chinese Academy of Geological Sciences, Beijing 100081, China
[b] Institute of Tibetan Plateau Research, Chinese Academy of Sciences, Beijing 100101, China

ARTICLE INFO

Article history:
Received 17 August 2015
Received in revised form 10 November 2015
Accepted 11 November 2015
Available online 5 January 2016

Handling Editor: Y.P. Dong

Keywords:
Granite
Laos
Zircon U–Pb age
Lu–Hf
Whole-rock major
Trace and rare earth elements

ABSTRACT

The Paleotethyan evolution of the Southeast Asia has become better understood in recent years. Questions remain, however, over the role of the Dien Bien Phu Suture Zone in the evolution of the Indochina Block and whether the Song Ma Suture represents the boundary between the Indochina Block and the South China Block. Granitoid geochronological and geochemical data obtained in northern Laos provide new information vis-à-vis these arguments. Zircon U–Pb ages together with whole rock, trace and rare earth element data from 27 granitic rocks from five complexes allow us to conclude that these granites are typical of I-type Indosinian volcanic arc granites. However, the 234–256 Ma I-type granites mismatch the initiation age obtained from the ductile shear zone of the Dien Bien Phu Fault, thus repudiating the existence of the Dien Bien Phu Suture Zone. This then implies that the Qamdo–Simao and Indochina blocks were united. The geochemical and geochronological data further suggest that the main crust in the Indochina Block formed in the Late Paleoproterozoic to Early Mesoproterozoic, much later than the Archean crustal formation age identified east of the Song Ma Suture. Moreover, the 440–404 Ma and 234–256 Ma I-type granites suggest that the boundary between Indochina and South China should be the Jinsha River Suture–Song Ma Suture–Kontum Massif, instead of the Jinsha River Suture–Song Chay Suture. Finally, the Emeishan basalt and granite complexes both form part of the South China tectonic units subducting westward under the Qamdo–Simao and Indochina blocks.

1. Introduction

Mainland Southeast Asia is formed of several micro-continents (e.g., the Sibumasu, Indochina, Qamdo–Simao and South China blocks) which amalgamated during the closure of the Paleotethyan Ocean from the Late Permian to the Early Triassic (e.g. Sengör, 1979; Metcalfe, 1996, 1999; Carter et al., 2001; Metcalfe, 2002; Ueno, 2003; Lepvrier et al., 2004; Ferrari et al., 2008; Lepvrier et al., 2008; Liu et al., 2012; Metcalfe, 2013; Faure et al., 2014). Though increasing level of details about the Paleotethyan evolution of the SE Asia has been defined in recent years, arguments remain about the welding of the blocks in Southeast Asia. For example, new studies have confirmed that the Changning–Menglian and Inthanon suture zones can be regarded as part of the Paleotethys Suture Zone, and that the Jinghong–Luang Prabang–Nan–Sra Kaeo Suture can be treated as a closed back-arc basin (e.g., Sone and Metcalfe, 2008; Metcalfe, 2013; Qian et al., 2015). However, uncertainty remains about the role of the Dien Bien Phu Suture (where the Dien Bien Phu fault is developed) in the Paleotethyan evolution of Southeast Asia (Fig. 1). Establishing this would help determine whether the Qamdo–Simao Block is part of the Indochina Block, or if the Indochina and the Qamdo–Simao blocks are two separate blocks. This question has perplexed geologists for a long time (e.g., Metcalfe, 1996; Wang et al., 2000; Carter et al., 2001; Metcalfe, 2002, 2006). One view insists that the Sukhothai Arc and the Inthanon Suture correlate with the Lincang–Jinghong Volcanic Belt and the Changning–Menglian Suture in Yunnan, China (e.g., Sone and Metcalfe, 2008; Metcalfe, 2013). Taking this view, the Qiangtang–Baoshan Block west of the Inthanon Suture would form the northern part of the Sibumasu Block, and the Qamdo–Simao Block east of the Suture would represent the northern continuity of the Indochina Block (e.g. Wang et al., 2000; Carter et al., 2001; Carter and Clift, 2008; Ferrari et al., 2008; Liu et al., 2012; Faure et al., 2014). However, others argue that the Nan Suture bends northeastward at the Dien Bien Phu Segment and joins the Song Ma Suture, separating the Nan Suture from the Changning–Menglian Suture by hundreds of kilometers (Sengör, 1979; Leloup et al., 1995; Singharajwarapan and Berry, 2000; Lepvrier et al., 2004, 2008). Another question concerns the time and geometry of plate convergence prior to collision between the Indochina and the South China blocks. Paleogeographic evidence suggests a connection between Indochina and South China up to the Carboniferous (e.g. Hutchison, 1989; Metcalfe, 1996; Janvier et al., 1997; Metcalfe, 2002; Racheboeuf et al., 2005, 2006; Metcalfe, 2013), but syn-tectonic magmatic and metamorphic data

* Corresponding author at: No. 11 Minzu Daxue Nan Rd, Haidian District, Beijing 100081, PR of China.
E-mail addresses: 948117360@qq.com, wsf@cags.ac.cn (S. Wang).

http://dx.doi.org/10.1016/j.gr.2015.11.011
1342-937X/

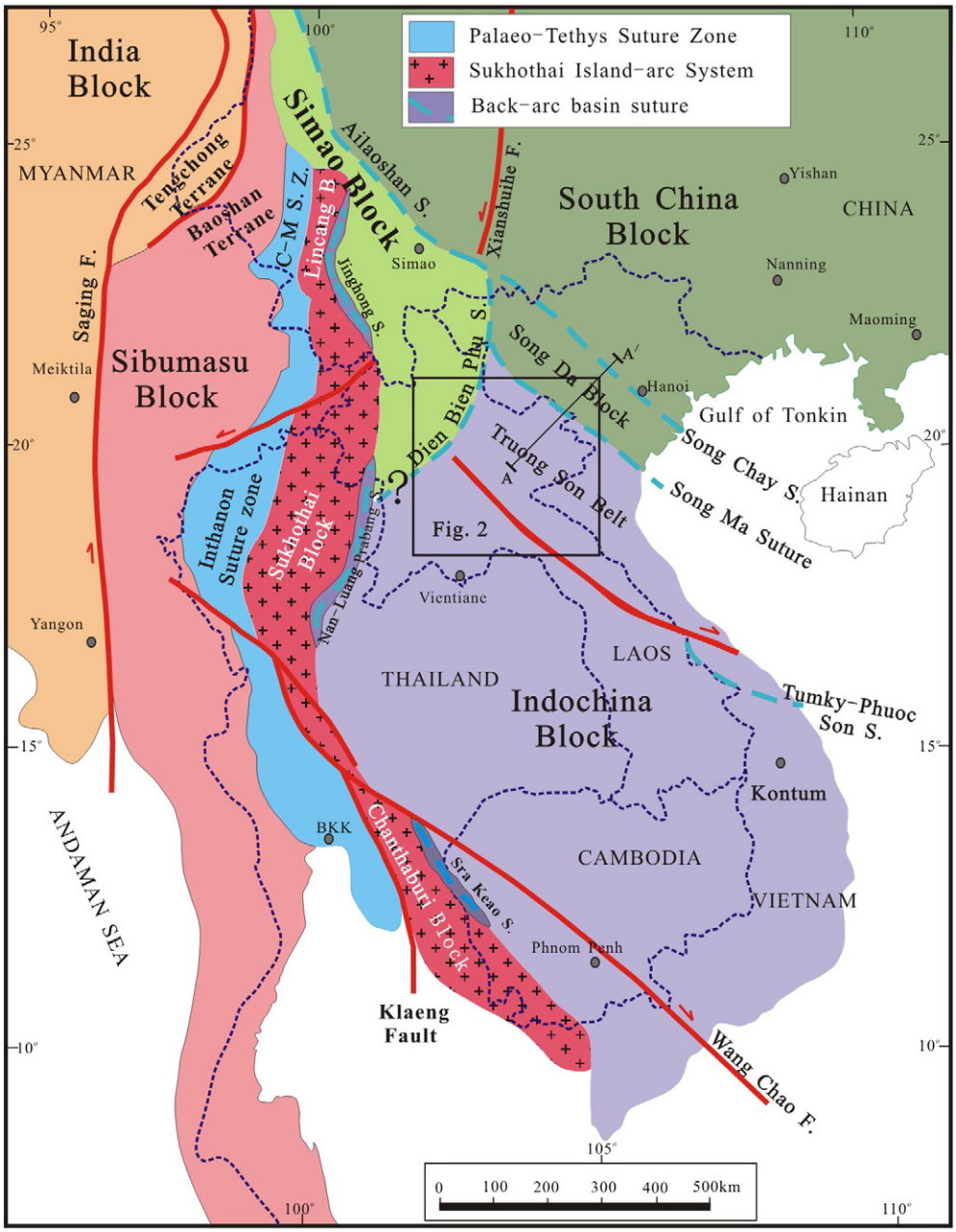

Fig. 1. Distribution of principal continental terranes and sutures of mainland Southeast Asia (after Sone and Metcalfe, 2008). CMSZ = Changning–Menglian Suture Zone; the locations shown in Figs. 2 & 3 are also shown.

show that a tectono-thermal event occurred between 260 Ma and 240 Ma (e.g. Lepvrier et al., 1997; Lan et al., 2000; Nagy et al., 2001; Lan et al., 2003; Lepvrier et al., 2004; Nakano et al., 2007; Owada et al., 2007; Lepvrier et al., 2008, 2011; Sanematsu et al., 2011; Lai et al., 2014). Additionally, varying opinions about the geometry of block convergence prior to collision exist, and include: 1) the eastward subduction of the Indochina Block beneath the South China Block (Lepvrier et al., 1997; Lan et al., 2000; Lepvrier et al., 2004); 2) the westward (or southward in a paleogeographic sense, as below) subduction of the South China Block beneath the Indochina Block (Liu et al., 2012; Faure et al., 2014); and 3) the existence of a pair of subduction zones dipping in opposite directions (Lepvrier et al., 2008).

Most areas of Laos are covered by virgin forest, which makes tracking the outcrops of the Dien Bien Phu ophiolitic suture difficult. Fortunately, granitoids are distributed broadly along the road from Phonsavan to Sam Neua in northern Laos, south of the junction between the Dien Bien Phu Suture and the Song Ma Suture (Fig. 2). It is widely accepted that the geochronological and geochemical data of granitic rocks can provide important information regarding the crustal evolution of tectonic plates. The geochronology and geochemistry of granitic rocks in northern Laos, however, are poorly known, due to their inaccessibility. In recent years we have collected more than 100 samples from different granitoid complexes in northern Laos in order to reconstruct the convergence processes of Southeast Asian blocks during the closure of the Paleotethyan Ocean.

2. Geological setting

2.1. The rocks in northern Laos

Proterozoic to Quaternary strata outcrop in central-northern Laos (Department of Geology and Mine, Lao P.D.R. (DGM), 1991; Fig. 2), and can be divided into three main units: Late Paleozoic, Early Mesozoic and Late Mesozoic. Late Paleozoic strata are mainly shallow sea-shelf

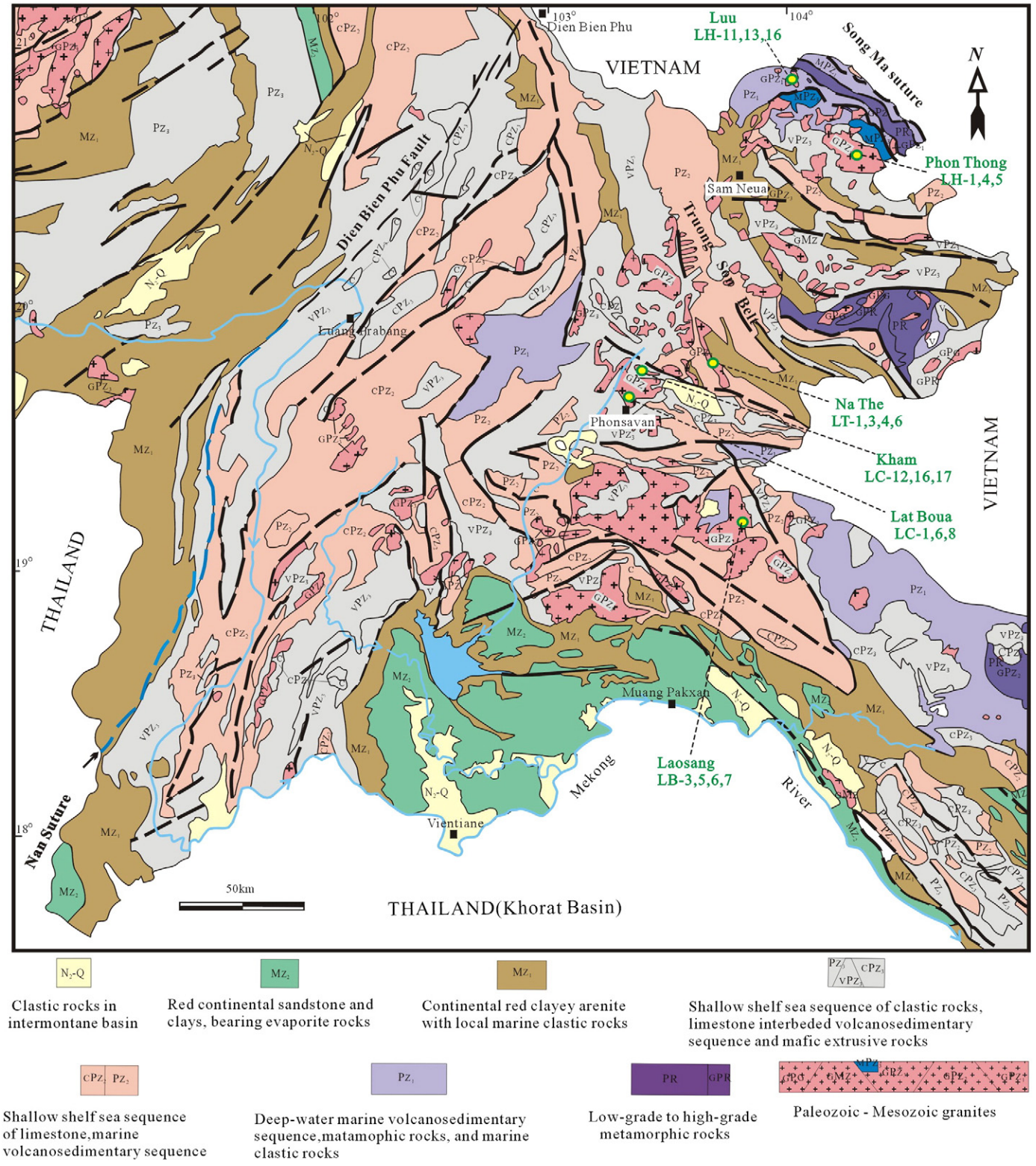

Fig. 2. Distribution of strata and granite complexes in northern Laos. Locations of granite samples are also shown (after DGM, 1991).

sequences interbedded with volcano-sedimentary sequences, mostly of sandstone, siltstone and shale. There are a few outcrops of Early Paleozoic rocks, which are mainly deep-water, marine volcano-sedimentary, metamorphosed to low or low-medium grades (DGM, 1991). Early Mesozoic strata are mostly of continental rock, with local shallow-water marine facies. Rocks in this unit are of red argillaceous sandstone, with occasional thin coal seams and conglomerates. These two stratigraphic units are distributed in a N–S direction. Late Mesozoic strata are mainly confined to the Vientiane Basin; rocks are mainly red continental sandstones and clays, with lagoonal mud rocks in the upper levels bearing halite and gypsum evaporate rocks. Granitoid complexes have developed on the Xieng Khoang Plateau of northern Laos (Fig. 2), which is located at the junction of the N–S trending granitoid belt in the Dien Bien Phu Segment of the Nan and Dien Bien Phu suture

zones, and the NW-striking Truong Son Belt. The granitoid belt along the Nan Suture has been interpreted being composed of syn-tectonic granitoids from the subduction of the Sibumasu Blockeastward into Indochina (e.g. Beckinsale et al., 1979; Charusiri et al., 1993; Barr et al., 2000). Conversely, the granitoids located along the northwestern extension of the Truong Son Belt have been attributed to the syn-tectonic or within-plate granitoids of the Indochina Block during its subduction eastward under the South China Block (e.g. Lepvrier et al., 1997, 2004; Sanematsu et al., 2011).

2.2. The tectonic setting around northern Laos

2.2.1. The Nan and Dien Bien Phu Suture Zones

The magmatic and sedimentary rocks in northern Laos are confined by two tectonic boundaries: the Nan-Dien Bien Phu Suture Zone in the west and northwest, and the Truong Son Belt in the east. The S–N striking Nan Suture Zone west of Laos consists of a belt of ophiolitic mafic and ultramafic rocks formed in a back-arc or inter-arc setting (Barr and MacDonald, 1987; Barr et al., 2000; Singharajwarapan and Berry, 2000), accompanied by the metasedimentary rocks of the Sukhothai Fold Belt, and syn-tectonic granite within what can be defined as a granite belt (Sone and Metcalfe, 2008). Northward, the Suture bends eastward and joins with the Song Ma Suture, thus separating the Indochina Block from the Qamdo–Simao Block (Sengör, 1979; Leloup et al., 1995; Singharajwarapan and Berry, 2000). Alternatively, the Nan Suture could be taken to connect northward with the Jinghong Suture in Yunnan, China (e.g., Barr and MacDonald, 1987; Wu et al., 1995; Barr et al., 2000; Sone and Metcalfe, 2008).

2.2.2. Tectonic units from Inner Indochina to the Red River Fault

The Song Ma Suture defines the boundary between the Indochina and South China blocks, although the Song Da or Song Chay sutures have also been considered the boundary (e.g. Lepvrier et al., 2004; Liu et al., 2012; Faure et al., 2014). Eastward, the tectonic units from Inner Indochina to South China can be subdivided into: the Indochina Basement; the Song Ma Suture Zone; the Nam Co Complex; the Song Da Rift Zone; the Tu Le Basin and the Song Chay Suture Zone (dissected by the Red River Fault (RRF) during the Cenozoic). The features of these tectonic units are described below; the relations between the units are shown as a simplified section in Fig. 3.

1) The Indochina Basement. Some high-grade metamorphic rocks and granite complexes in northern Laos and northwestern Vietnam are attributed to the Archean to Proterozoic eons (DGM, 1991; Department of Geological and Minerals of Vietnam (DGMV), 2005), similar to the basement of the Kontum Massif in the southernmost part of Vietnam (e.g. Osanai et al., 2001, 2004; Nakano et al., 2007; Owada et al., 2007; Sanematsu et al., 2011).
2) The Song Ma Suture Zone, which is composed of the Song Ca volcanic arc, the Truong Son Belt (Truong Son arc granitoids) and the Song Ma tectonic mélange, from W–E. The Song Ca volcanic arc is comprised mainly of a sequence of calcalkaline volcanic associations of ages 270–248 Ma, using $^{40}Ar/^{39}Ar$ dating (Lan et al., 2003). The Truong Son Belt consists of widespread Late Paleozoic to Early Mesozoic intrusions. Truong Son Belt strata exhibit: Neoproterozoic high-grade metamorphic rocks; Silurian to Lower Devonian and Upper Permian marine sedimentary rocks; Upper Permian basalt, amygdaloidal basalt and tuffs; and Triassic marine and terrigenous sedimentary rocks. The Song Ma mélange is defined as the boundary between the Indochina and South China blocks that occurred during the westward subduction of the South China Sea under the Indochina Block in the Later Permian to Early Triassic (e.g. Lepvrier et al., 2004, 2008; Liu et al., 2012; Faure et al., 2014). It consists of sheets of rocks with ages from Neoproterozoic to Early Triassic. These rocks are highly sheared, juxtaposed by shear zones and intruded by gabbro, plagiogranite, granodiorite and granite (DGMV, 2005).
3) The Nam Co Complex is a high-grade metamorphic massif. Proterozoic greenschist to amphibolite facies metamorphic rocks, including gneisses, schists, amphibolites, quartzite and marbles constitute the majority of the Massif. The metamorphic rocks are highly foliated and lineated, and were formed ~245 Ma (Lepvrier et al., 2004).
4) The Song Da Rift Zone. The lowermost sequence is composed of Lower Permian carbonates overlain by a sequence of mafic to ultramafic volcanic rocks of the Lower Permian Cam Thuy Formation. The middle sequence is Upper Permian to Early Triassic, and is composed of an association of komatiite-basalt, trachytic basalt, trachytic andesite and trachytic dacite. Upward, the sequence exhibits calcareous sediments interlayered with felsic volcanics in its Mid to Late Triassic sediments. The top sequence is Cretaceous sedimentary rocks unconformably overlying old sequences. East of the Song Da Rift Zone is the Tu Le Basin, which is filled with Mesozoic continental sediments. East of the Tu Le Basin is the Song Chay Suture Zone, which includes the Song Chay ophiolitic mélange and the Day Nui Con Voi (DNCV) gneiss belt, where the Red River Fault dissected the mélange during the Cenozoic.

The Indochina Block has been thoroughly overprinted and cut by Neogene strike-slip faults such as the Ailaoshan–Red River Fault, the Wangchao Fault and the Dien Bien Phu Fault. The NE-trending Dien Bien Phu Fault in our study area appears to have been the southernmost segment of the Xianshuihe fault system during the Late Cenozoic; the Fault has been an active left-lateral strike slip fault since ~5.5 Ma, and

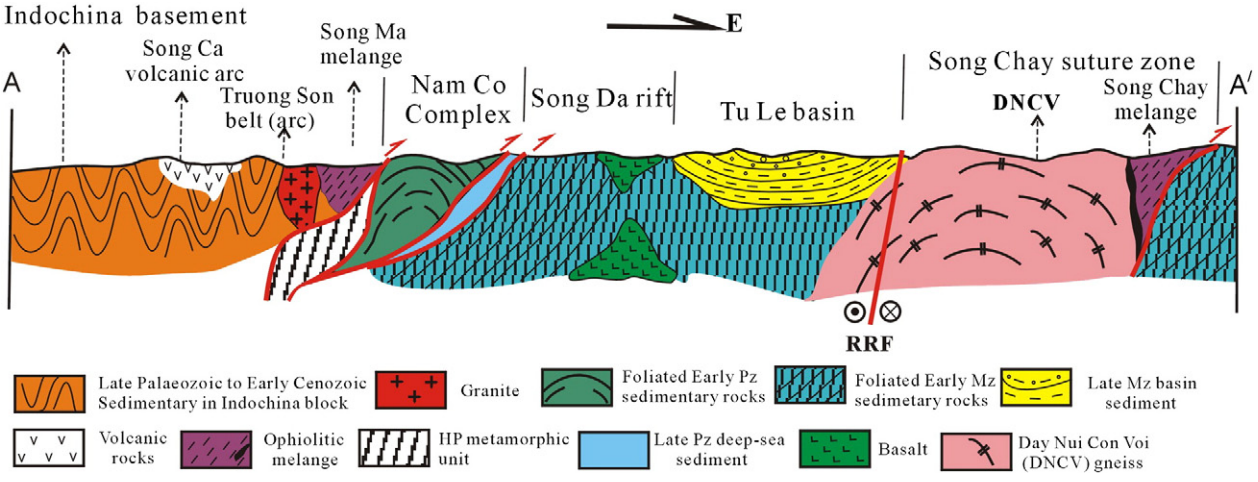

Fig. 3. Cross-section of the Song Ma Suture Zone shows the simplified geological relation between different tectonic units eastward from the Indochina Block to the South China Block.

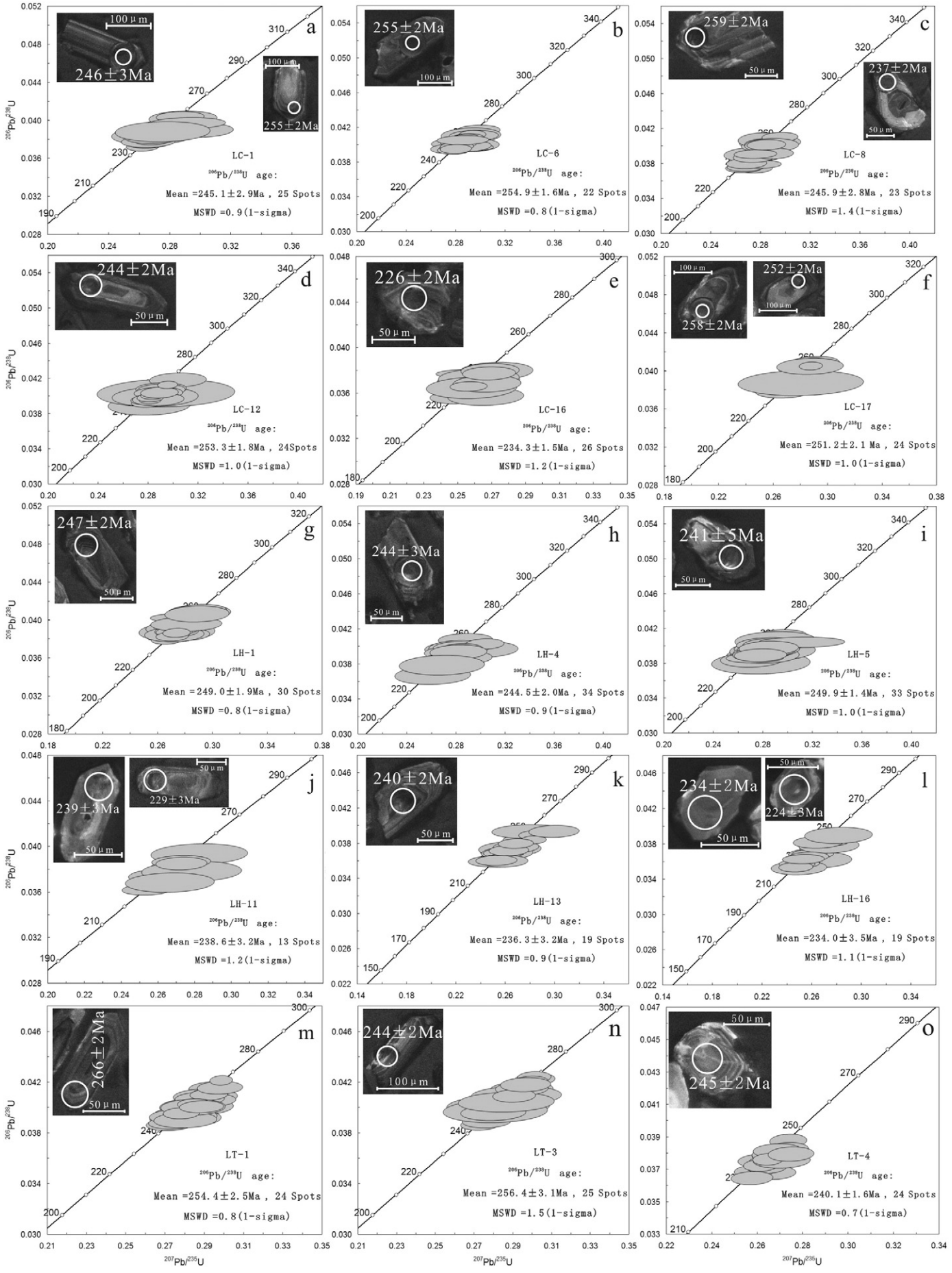
a
246±3Ma
255±2Ma
LC-1
Mean =245.1±2.9Ma , 25 Spots
MSWD =0.9(1-sigma)
b
255±2Ma
LC-6
Mean =254.9±1.6Ma , 22 Spots
MSWD =0.8(1-sigma)
c
259±2Ma
237±2Ma
LC-8
Mean =245.9±2.8Ma , 23 Spots
MSWD =1.4(1-sigma)
d
244±2Ma
LC-12
Mean =253.3±1.8Ma , 24Spots
MSWD =1.0(1-sigma)
e
226±2Ma
LC-16
Mean =234.3±1.5Ma , 26 Spots
MSWD =1.2(1-sigma)
f
252±2Ma
258±2Ma
LC-17
Mean =251.2±2.1 Ma , 24 Spots
MSWD =1.0(1-sigma)
g
247±2Ma
LH-1
Mean =249.0±1.9Ma , 30 Spots
MSWD =0.8(1-sigma)
h
244±3Ma
LH-4
Mean =244.5±2.0Ma , 34 Spots
MSWD =0.9(1-sigma)
i
241±5Ma
LH-5
Mean =249.9±1.4Ma , 33 Spots
MSWD =1.0(1-sigma)
j
239±3Ma
229±3Ma
LH-11
Mean =238.6±3.2Ma , 13 Spots
MSWD =1.2(1-sigma)
k
240±2Ma
LH-13
Mean =236.3±3.2Ma , 19 Spots
MSWD =0.9(1-sigma)
l
234±2Ma
224±3Ma
LH-16
Mean =234.0±3.5Ma , 19 Spots
MSWD =1.1(1-sigma)
m
266±2Ma
LT-1
Mean =254.4±2.5Ma , 24 Spots
MSWD =0.8(1-sigma)
n
244±2Ma
LT-3
Mean =256.4±3.1Ma , 25 Spots
MSWD =1.5(1-sigma)
o
245±2Ma
LT-4
Mean =240.1±1.6Ma , 24 Spots
MSWD =0.7(1-sigma)
206Pb/238U
207Pb/235U
206Pb/238U age:

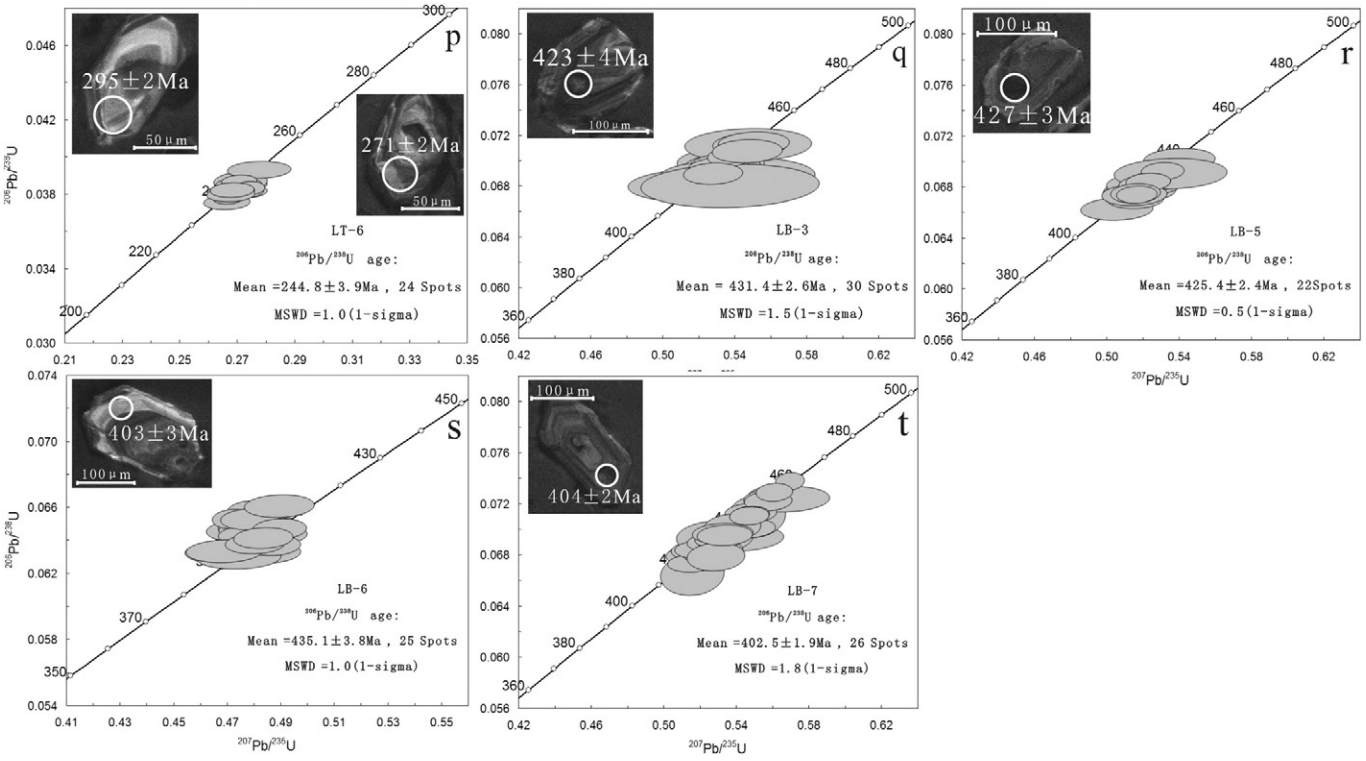

Fig. 4. Cathodoluminescence (CL) images of representative zircon grains and zircon age concordia diagrams of granites from northern Laos.

reactivated after 228 Ma or 198–158 Ma, with a total right-lateral offset accumulation of 30–40 km (e.g. Wang et al., 1998; Zuchiewicz et al., 2004; Koszowska et al., 2007; Lin et al., 2009; Roger et al., 2014).

3. Analytical methods

About 24 granite samples were prepared for zircon U–Pb LA-ICP-MS dating. Zircons were separated using conventional heavy-liquid and magnetic techniques. Pure zircon grains were selected using a binocular microscope. Representative grains were placed into an epoxy resin, along with several standard transmission electron microscopy (TEM) samples, and ground down by about half to expose the zircon interior, before performing U–Pb dating. Before and after the dating, transmitted and reflected light were analyzed using a microscope and backscattering images, together with cathode luminescence images, in order to determine crystalline shape, inner structure and dating position.

U–Pb dating of zircons was conducted using a New Wave UP193FX Excimer laser, coupled with an Agilent 7500a ICPMS, at the Key Laboratory of Continental Collision and Plateau Uplift, Institute of Tibetan Plateau Research, Chinese Academy of Sciences (CAS), Beijing. The diameter of the laser beam was 36 mm, and the duration of ablation was 45 s. Zircon standard 91500 was used as an external standard to correct isotopic ratios. TEM characterization of zircon was used to monitor results. Concentrations of the elements were calculated using NIST612 glass as the external standard and ^{29}Si as the internal standard. Age data were processed using Glitter 4.4 software (details can be found in Jackson et al., 2004). Diagrams were produced using the Isoplot 3.0 Toolkit (Ludwig, 2003).

In-situ Hf isotope analysis was performed on zircon grains using LAICPMS with a beam size of 60 μm and a laser pulse frequency of 8 Hz. Details of instrument conditions and data acquisition are given in Wu et al. (2006) and Xie et al. (2008). During the analysis, $^{176}Hf/^{177}Hf$ ratios of the zircon standard (91500) were measured as 0.282286 ± 12 (2σ, n = 21). The εHf(t) values (parts in 104 deviations in initial Hf isotope ratios between the zircon sample and the chondritic reservoir) and T_{DM2} values (zircon Hf isotope crustal model ages based on a depleted-mantle source and an assumption that the protolith of the zircon's host magma has a mean continental crustal $^{176}Lu/^{177}Hf$ ratio of 0.015) were calculated following Griffin et al. (2002), using the ^{176}Lu decay constant given in Blichert-Toft and Albarède (1997).

About six granite samples were chosen for whole-rock major, rare earth and trace element analyses. Samples for elemental analysis were powdered to <20 μm using an agate mill. Major element analyses were conducted at the Institute of Geology and Geophysics, CAS. Major element abundances (wt.%) of whole-rock samples were determined using a Phillips PW X-ray fluorescence spectrometer (XFR-2400), and yielded an analytical uncertainty of <5% (±1σ). Rare earth and other trace elements were analyzed using ICP-MS techniques at the Institute of Tibetan Plateau Research, CAS. The detailed operating conditions for the laser ablation system, the ICP-MS instrument and data reduction are the same as those described by Liu et al. (2008), with the uncertainties for all elements <5%.

4. Results

4.1. U–Pb dating

More than 40 samples from six granite complexes along the road from Phonsavan to Sam Neua in northern Laos were selected for zircon analysis. ~20 representative samples are presented in this paper to show the geochronology of the complexes. The samples collected are termed LC-1, LC-6 and LC-8 (from the Lat Boua Complex); LC-12, LC-16 and LC-17 (from the Kham Complex); LH-1, LH-4 and LH-5 (from the Phon Thong Complex); LH-11, LH-13 and LH-16 (from the Luu Complex); LT-1, LT-3, LT-4 and LT-6 (from the Na The Complex); and LB-3, LB-5, LB-6 and LB-7 (from the Laosang Complex) (Fig. 2). The sites of the complexes are located between 19°41.396′N and 20°49.650′N and between 103°28.176′E and 104°19.781′E. Of the six complexes, the Lat Boua, Kham, Phon Thong, Luu and Na The complexes exhibit ages ~234–256 Ma; the Laosang Complex gives a mean age of 420 Ma (Fig. 4, Table 1 in Appendix A). Only a few zircons from some

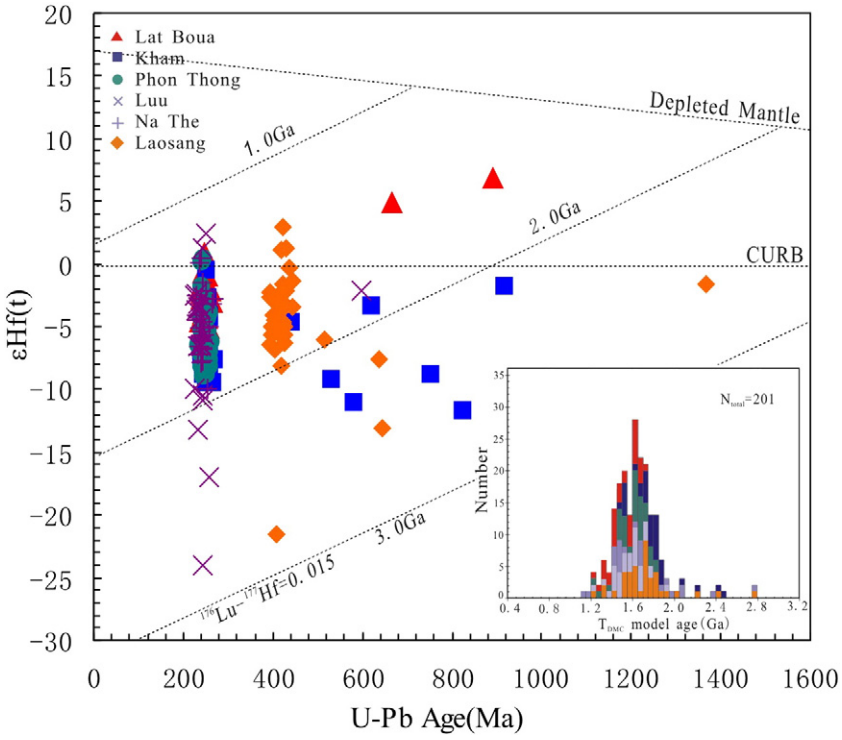

Fig. 5. Plot of εHf(t) vs. U–Pb ages for granites from northern Laos.

samples show the existence of inherited cores, as described in Section 4.2 and Table 2 in Appendix B.

Zircons from the 16 samples from the Lat Boua, Kham, Phon Thong, Luu and Na The complexes are mainly light yellow to transparent, euhedral prismatic grains. Cathode luminescence images (CL) show that these zircons generally have luminescent (low U) cores with euhedral fine-scale oscillatory igneous zoning. They generally range from 120 to 200 μm in length and 50–80 μm in width. As a rule, we selected 25–35 representative zircons from these 16 samples for U–Pb dating (Table 1 in Appendix A). Th/U ratios range from 0.18 to 1.58, indicating a typical magmatic origin. Analytical results are generally grouped together and yield weighted mean $^{206}Pb/^{238}U$ ages ranging from 234.3 ± 1.5 Ma to 256.4 ± 3.1 Ma (95% confidence; MSWD values range from 0.9 to 1.5) (Fig. 4), which we therefore interpreted as the

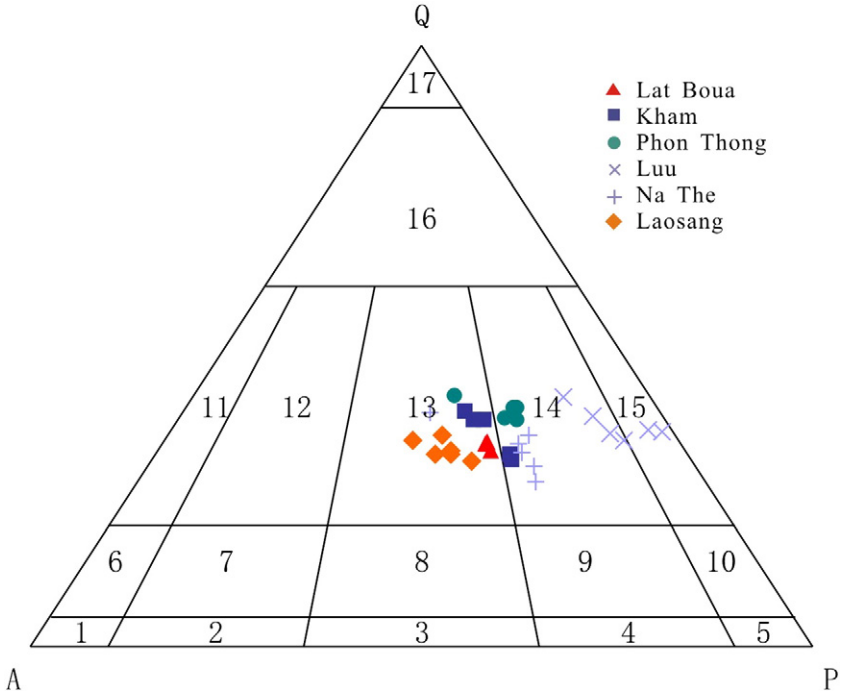

Fig. 6. Modal classification of granitoids (after Streckeisen, 1967). Granites from the Lat Boua, Laosang and Kham complexes fall mainly in the monzogranite field; granites from the Phon Thong, Na The, and Luu complexes are in the granodiorite field; two samples from the Luu complex fall into the tonalite field. 1 — alkali feldspar syenite; 2 — syenite; 3 — monzonite; 4 — monzodiorite; 5 — diorite; 6 — quartz alkali feldspar syenite; 7 — quartz syenite; 8 — adamellite; 9 — quartz monzobiorite; 10 — quartz diorite; 11 — alkalic feldspar granite; 12 — syengranite; 13 — monzogranite; 14 — granodiorite; 15 — tonalite; 16 — quartz granite; 17 — quartzite.

Table 4
Whole-rock major element components in the 33 samples extracted from six complexes in northern Laos.

	Lat Boua	Kham	Na The	Phon Thong	Luu	Laosang
SiO_2 (%)	71–71.8	64.6–73.9	68.4–77.5	73.4–74.3	72.9–75.0	69.2–71.6
$Na_2O + K_2O$ (%)	7.24–7.41	7.1–7.8	7.0–8.1	6.4–7.1	6.3–7.2	7.4–7.9
K_2O/Na_2O	1.15–1.19	1.23–1.35	0.78–1.53	0.8–1.36	0.03–0.39	1.39–2.11
Al_2O_3 (%)	14.5–14.8	12.8–14.8	12.8–15.9	12.6–13.0	11.4–12.5	14.0–15.5
Aluminum index	1.04–1.08	1.0–1.04	1.03–1.05	0.96–1.12	0.78–1.03	1.06–1.08
Litman index	1.87–1.96	1.50–1.63	1.61–2.28	1.32–1.59	1.22–1.75	1.92–2.24
Granites	Monzogranite	Monzogranite	Granodiorite	Granodiorite	Tonalite	Monzogranite
Alkalinity	High-K calc-alkaline	High-K calc-alkaline	High-K calc-alkaline	Calc-alkaline	Low-K	High-K calc-alkaline
Aluminum	Peraluminous	Peraluminous	Peraluminous	Meta-aluminous	Meta-aluminous	Peraluminous

crystallization ages of the Lat Boua, Kham, Phon Thong, Luu and Na The complexes.

The Laosang granite complex, where samples LB-3, LB-5, LB-6 and LB-7 were collected, is located at approximately 19°13.872′N, 103°40.482′E. Zircons from samples LB-3, LB-5, LB-6 and LB-7 consist of light yellow to transparent, euhedral prismatic grains. CL images show that these zircons generally have luminescent (low U) cores with euhedral fine-scale oscillatory igneous zoning. They generally range from 120 to 180 μm in length and from 50 to 80 μm in width. Zircon characteristics are similar to those of zircon from the other five complexes. We selected 30, 22, 25 and 26 representative zircons respectively from the four samples for U–Pb dating (Table 1 in Appendix A). The Th/U ratios ranged from 0.18 to 1.58, 0.20 to 2.06, 0.16 to 1.30 and 0.18 to 0.76, respectively, indicating typical magmatic origins. Analytical results are generally grouped together and yield a weighted mean $^{206}Pb/^{238}U$ age of 431.4 ± 2.6 Ma (95% confidence, MSWD = 1.5) for LB-3; 425.4 ± 2.4 Ma for LB-5 (95% confidence, MSWD = 0.5); 435.1 ± 3.8 Ma for LB-6 (95% confidence, MSWD = 1.0); and 402.5 ± 1.9 Ma (95% confidence, MSWD = 1.8) for LB-7 (Fig. 4q, r, s, t). We interpreted these values as representative of the crystallization ages of the Laosang granite complex.

4.2. Zircon Lu–Hf isotopic data

We selected a total of 12 samples, i.e., LC-1, LC-8, LC-12, LC-17, LH-4, LH-5, LH-11, LH-16, LT4, LT6, LB-5 and LB-7, for in-situ Lu–Hf isotopic analyses based on zircon U–Pb dated samples of the six complexes described in Section 4.1. Approximately 15–20 spots in each sample (201 spots in total) were selected for analysis. The results are listed in Table 2 in Appendix B, and are shown in Fig. 5.

The 31 analyses of protogenetic magmatic zircon from the Lat Boua Complex display initial $^{176}Hf/^{177}Hf$ ratios ranging from 0.282075 to 0.282644, and εHf(t) values from −19.1 to 0.9, with only spot LC-8-6 having a positive εHf(t) value. Corresponding Hf crustal two stage model ages (T_{DM2}) range from 1218 Ma to 1701 Ma, with a mean of 1526 Ma. The 29 analyses of young U–Pb ages from the Kham Complex display initial $^{176}Hf/^{177}Hf$ ratios ranging from 0.282336 to 0.282604 and εHf(t) values from −9.5 to −0.5; corresponding Hf crustal T_{DM2} ages range from 1218 Ma to 1701 Ma, with a mean of 16,984 Ma. The 37 analyses from the Phon Thong Complex display initial $^{176}Hf/^{177}Hf$ ratios ranging from 0.282369 to 0.282632, εHf(t) values from −8.9 to 0.4, and Hf crustal T_{DM2} ages from 1245 Ma to 1835 Ma, with a mean of 1606 Ma. 21 spots from the Luu Complex show initial $^{176}Hf/^{177}Hf$ ratios ranging from 0.281943 to 0.282687 and εHf(t) values from −24.0 to 2.5, with only spot LH-4-13 having a positive εHf(t) value; Hf crustal T_{DM2} ages range from 1120 Ma to 2789 Ma, with a mean of 1679 Ma. The 33 isotopic analyses of the Na The Complex display initial $^{176}Hf/^{177}Hf$ ratios ranging from 0.282333 to 0.282636 and εHf(t) values from −9.9 to 0.5 (only spot LT-4-18 has a positive value), with a mean value of −4.6; Hf crustal T_{DM2} ages range from 1240 Ma to 1909 Ma, with a mean of 1574 Ma. The 38 analyses from the Laosang Complex display initial $^{176}Hf/^{177}Hf$ ratios ranging from 0.282283 to 0.282540, εHf(t) values from −8.1 to 1.2 (only spot LB-5-17 has a positive value), and Hf crustal T_{DM2} ages from 1220 Ma to 2751 Ma, with a mean of 1678 Ma. These Lu–Hf isotopic features obtained from protogenetic magmatic zircons indicate that the rock formations of the complexes were principally sourced from Late Paleoproterozoic to Early Mesoproterozoic continental crust, with a minute quantity from the depleted mantle.

Besides the analyses of protogenetic magmatic zircons, Hf crustal T_{DM2} ages were recorded using inherited zircons from four complexes, i.e., the Lat Boua, Kham, Luu and Laosang complexes. The U–Pb ages of two inherited zircons from spots LC-8-2 and LC-8-15 in the Lat Boua Complex are 667 Ma and 892 Ma, respectively; their $^{176}Hf/^{177}Hf$ ratios

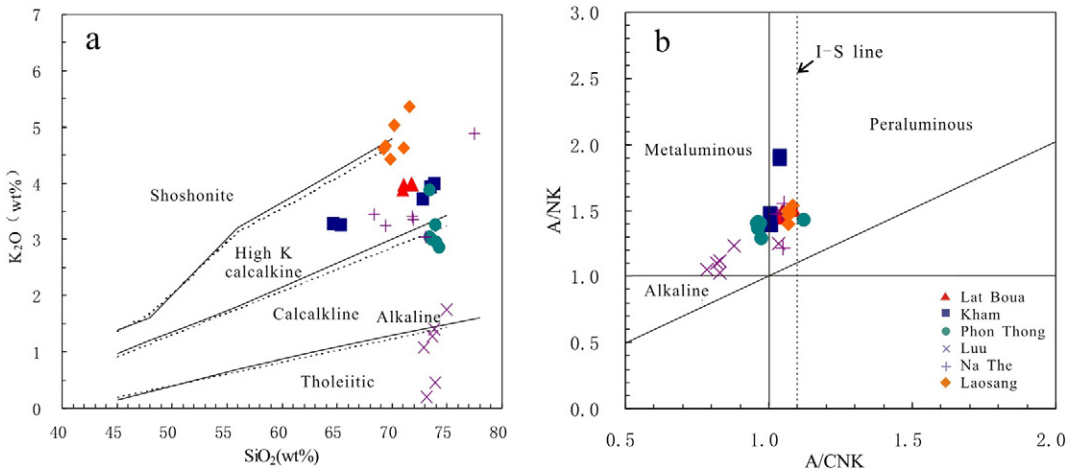

Fig. 7. Plots of (a) K_2O vs. SiO_2 (solid line after Peccerillo and Taylor, 1976; dashed line after Middlemost, 1985) and (b) A/NK vs. A/CNK (after Maniar and Piccoli, 1989) for granites from northern Laos. A = Al_2O_3, N = Na_2O, K = K_2O, C = CaO (all in molar proportion).

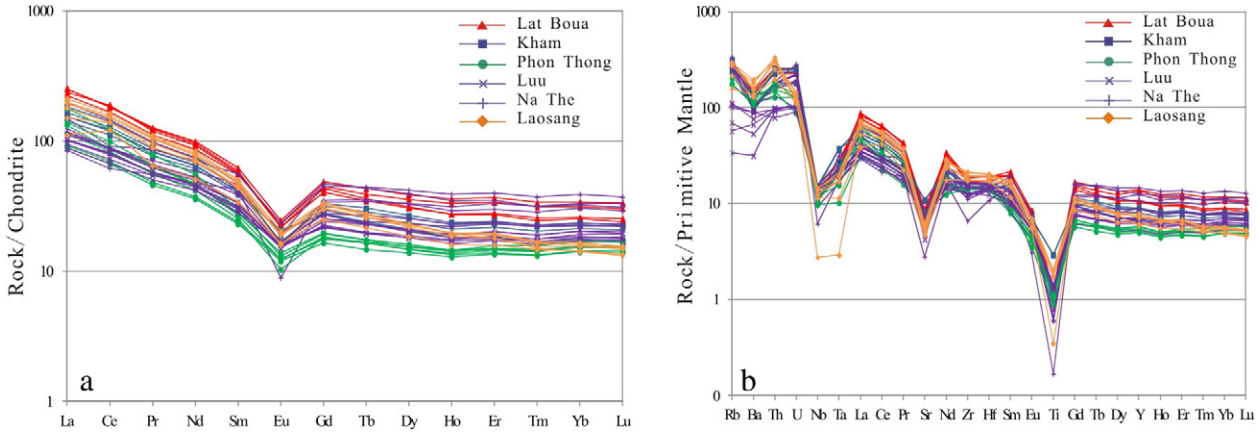

Fig. 8. Chondrite-normalized REE patterns (Boynton, 1984) and primitive-mantle normalized trace element patterns for I-type granites in northern Laos (Sun and McDonough, 1989).

are 0.282844 and 0.282944, their εHf(t) values are 4.9 and 6.8, and they exhibit corresponding T_{DM2} values of 1336 and 1288 Ma, respectively. In the LC-12 sample from the Kham Complex, the U–Pb ages of two inherited zircons from spots LC-12-6 and LC-12-12 are 530 Ma and 580 Ma, respectively; their $^{176}Hf/^{177}Hf$ ratios are 0.282366 and 0.282049, their εHf(t) values are −9.2 and −11.0, and they give corresponding T_{DM2} values of 2070 and 2222 Ma, respectively. In the LC-17 sample, the U–Pb ages of the five inherited zircons are 440 Ma, 750 Ma, 618 Ma, 822 Ma and 915 Ma, respectively; their $^{176}Hf/^{177}Hf$ ratios range from 0.282140 to 0.282573, their mean εHf(t) value is −6.0, and their corresponding T_{DM2} values lie between 1710 Ma and 2446 Ma. In the LB-5 sample from the Laosang Complex, the U–Pb ages of three inherited zircons from spots LB-5-6, LB-5-16 and LB-5-19 are 645 Ma, 1367 Ma and 515 Ma respectively; their $^{176}Hf/^{177}Hf$ ratios are 0.282103, 0.282453 and 0.282345, their εHf(t) values are −13.1, −1.7 and −6.0, and their corresponding T_{DM2} values are 1860, 2233 and 2408 Ma, respectively. In the LB-7 sample, the U–Pb age of the inherited zircon is 636 Ma, its $^{176}Hf/^{177}Hf$ ratio is 0.282411, its mean εHf(t) value is −7.7, and its corresponding T_{DM2} value is 2054 Ma. All the Lu–Hf isotopic features obtained from inherited zircons indicate that the complexes are sourced at least partly by Late Paleoproterozoic to Early Mesoproterozoic continental crust and depleted mantle, with a minute quantity coming from the Archeozoic lower crust.

4.3. Whole-rock major, trace and rare earth element data

33 granitic samples were collected from the six complexes for major, trace and rare earth element (REE) analyses (Table 3 in Appendix C). As seen in the QAP diagram (Fig. 6) (Streckeisen, 1967), granitic rocks from the Lat Boua, Kham and Laosang complexes fall into the monzogranite field. Granites from the Phon Thong and Na The complexes, as well as four samples from the Luu Complex, fall into the granodiorite field. Two samples from the Luu Complex fall into the tonalite field. All the samples have similar SiO_2, $Na_2O + K_2O$ and Al_2O_3 contents, but their

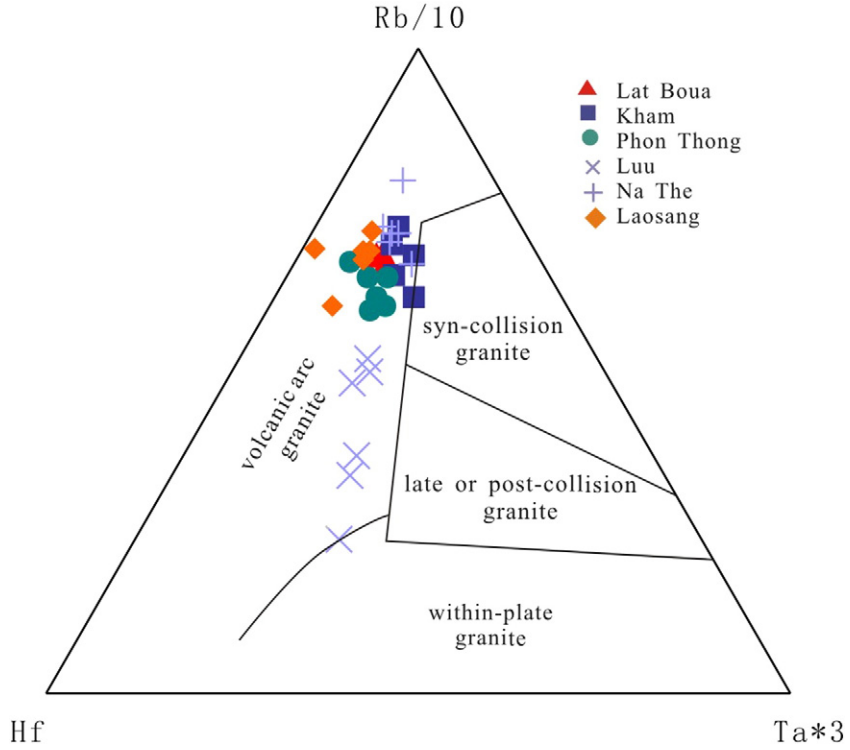

Fig. 9. Hf–Rb–Ta discrimination diagram (Harris et al., 1986), identifying tectonic setting.

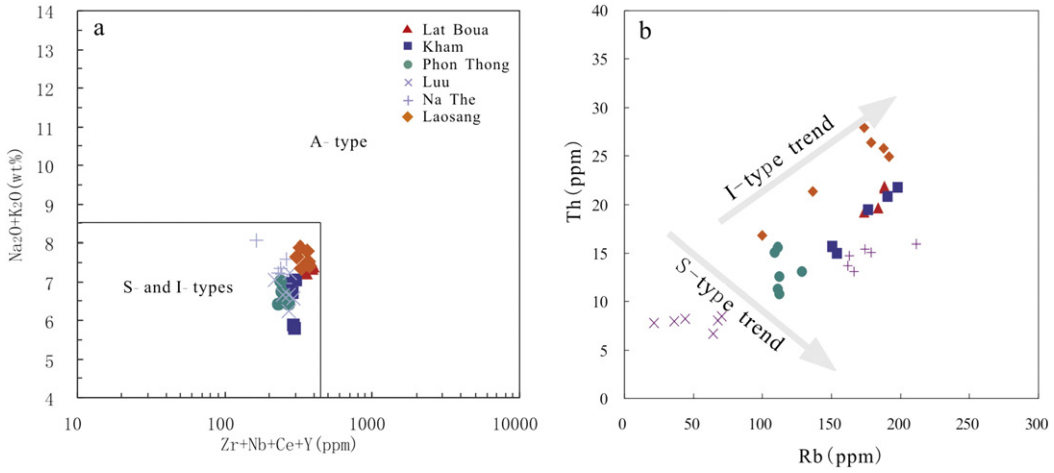

Fig. 10. ($Na_2O + K_2O$) vs. (Zr + Nb + Ce + Y) diagram (Whalen et al., 1987) and Th vs. Rb diagram (Chappell and White, 1992), identifying I–S type granites.

K_2O/Na_2O ratios and aluminum indices (A/CNK) vary in different complexes (Table 4). Thus, in the K_2O vs. SiO_2 and A/NK vs. A/CNK diagrams (Fig. 7) (Peccerillo and Taylor, 1976; Middlemost, 1985; Maniar and Piccoli, 1989), samples from the Lat Boua, Kham, Na The and Laosang complexes all fall into the peraluminous high-K calcalkaline field, but samples from the Phon Thong and Luu complexes fall into the meta-aluminous calcalkaline or meta-aluminous low-K fields.

Granite samples from the six complexes display similar patterns in the chondrite (Boynton, 1984) and primitive mantle (Sun and McDonough, 1989) normalized rare earth and trace element plots. All rocks show enriched light rare earth element (LREE) and flat heavy rare earth element (HREE) chondrite-normalized REE patterns (Fig. 8a), with the LREE/HREE ratio between 6.38 and 8.06 in the Lat Boua Complex; between 6.87 and 7.83 in the Kham Complex; between 6.25 and 10.37 in the Phon Thong Complex; between 5.30 and 9.48 in the Luu Complex; between 3.05 and 4.76 in the Na The Complex; and between 7.89 and 9.97 in the Laosang Complex. The La_N/Yb_N ratio ranges from 7.19 to 10.03 in the Lat Boua Complex; from 7.23 to 8.80 in the Kham Complex; from 5.94 to 11.87 in the Phon Thong Complex; from 5.09 to 10.67 in the Luu Complex; from 2.78 to 4.70 in the Na The Complex; and from 7.73 to 15.07 in the Laosang Complex. Eu negative anomalies are observed, with mean σ Eu ranging from 0.49 to 0.56. The rocks have similar patterns in the chondrite (Boynton, 1984) and primitive mantle (Sun and McDonough, 1989) normalized rare earth and trace element plots, marked by variable enrichments in Rb, Ba, Th and Ce, and depletions in Ta, Nb, Sr and Ti (Fig. 8b). Furthermore, the Sr values from all the samples are ~100–330 ppm, other than for LH-14, which is 89 ppm, and LT-7 and LB-4, which are as low as 58.7 ppm. Yb values are <2 ppm. The granite shows low Sr and Yb contents, indicating that the magmatic source of the granite contained relics of plagioclase and garnet. The original rocks are plagioclase and garnet high-pressure metamorphic rocks. Additionally, in the Th/Yb vs. Ta/Yb and Hf–Rb–Ta tectonic classification diagrams (Fig. 9) (Harris et al., 1986), all the granitic rocks fall into the volcanic arc granite field, and

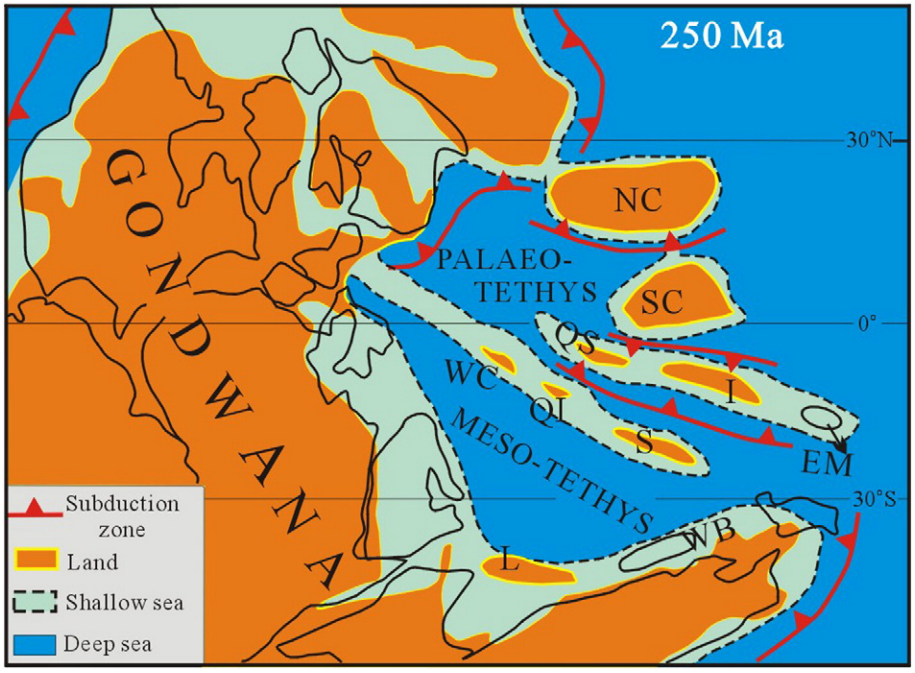

Fig. 11. Paleogeographic reconstructions of the Tethyan region in the Late Permian to Early Triassic, showing relative positions of the East and Southeast Asian blocks and distribution of land and sea (after Metcalfe, 2006). Abbreviations: SC = South China; NC = North China; I = Indochina; QS = Qamdo–Simao; EM = East Malaya; S = Sibumasu; WB = West Burma; QI = Qiangtang; L = Lhasa; WC = Western Cimmerian Continent.

are classified as I-type granites in the (Na_2O + K_2O) vs. (Zr + Nb + Ce + Y) and Th vs. Rb diagrams (Fig. 10) (Whalen et al., 1987; Chappell and White, 1992). Overall, the whole-rock major, trace and rare earth element characteristics of the 33 granites from the six complexes are typical of I-type volcanic arc granites.

5. Discussion

5.1. Crustal characteristics of the Indochina Block

According to the zircon U–Pb ages from northern Laos (Section 4.1), the Indochina Block experienced two periods of magmatic activity from the Early Paleozoic to the Early Mesozoic. One lasted from 402.5 Ma to 435.1 Ma, and the second from 234.3 Ma to 256.4 Ma. Additionally, some inherited zircon cores disclose the occurrence of magmatic intrusion from the Early Paleozoic to the Late Paleoproterozoic. Inherited zircon grains from the same Indochina Block in Malaysia, in addition to the Kontum Massif, also exhibit Proterozoic ages (800 Ma, 1200 Ma, 1350 Ma, 1403 Ma, 1600 Ma, 1800 Ma and 2600 Ma) (Liew and McCulloch, 1985; Carter et al., 2001; Nagy et al., 2001). Furthermore, detrital zircon ages from the Indochina Block also suggest that basement metasedimentary rock protoliths were formed during the Meoproterozoic–Early Paleozoic (Burrett et al., 2014): this differs from the Archean basement age (3.5–2.7 Ga) obtained from central Vietnam, east of the Song Ma Suture (Lan et al., 2001, 2003).

Moreover, the T_{MD2} ages for Late Permian to Early Triassic granites mainly range from 1511 Ma to 1621 Ma in the Lat Boua Complex; 1670 Ma to 1718 Ma in the Kham Complex; 1598 Ma to 1613 Ma in the Phon Thong Complex; 1735 Ma to 1782 Ma in the Luu Complex; and 1565 Ma to 1584 Ma in the Na The Complex. The T_{MD2} ages of some spots fall within the 2500–2000 Ma period, and only a few spots render modeled ages older than 2500 Ma. The T_{MD2} ages of Early Paleozoic granites (Laosang Complex) are ~1702–1760 Ma. The εHf(t) values of the 12 samples are almost all negative, with mean εHf(t) values ranging from −3.4 to −8.2, indicating that these samples were sourced principally by re-melted crust. Only a few spots have positive εHf(t) values, indicating a depleted mantle source.

Zircon inheritance ages and T_{MD2} ages suggest that the main crust of the Indochina Block was formed in the Late Paleoproterozoic to Early Mesoproterozoic, and that the role of Archean rocks in the crustal evolution of the Indochina Block was limited. This conclusion is similar to observations from the Kontum Massif (Carter et al., 2001; Nagy et al., 2001), and in the East Coast Province batholiths of the Malaysian Peninsula (Liew and McCulloch, 1985), located in the southwestern part of the Indochina Block. The ages are much younger than those obtained in the Cavinh Complex of northern Vietnam, which is Archean (Lan et al., 2001). The differences in crustal evolution between the Indochina Block and the block east of the Song Ma Suture further confirm that the boundary between Indochina and South China can be taken as the Song Ma Suture (Lepvrier et al., 2004; Liu et al., 2012; Faure et al., 2014), not the Song Da or Song Chay sutures, as once assumed.

5.2. A single Qamdo–Simao–Indochina Block

Overall, the characteristic patterns exhibited by whole-rock major, trace and rare earth element data from the six plutons are typical of I-type volcanic arc granites (Section 4.3; Figs. 6–10). This result is similar to data from the Dien Bien granite massif west of the Song Ma Suture (Lan et al., 2001; Liu et al., 2012; Roger et al., 2014). The granites located at the junction of the Dien Bien Phu and Song Ma sutures, and once attributed to the Sibumasu–Simao Block, clearly subducted eastward under the Indochina Block along the Dien Bien Phu Suture. Sengor (1984) named the Dien Bien Phu Suture the "Dien Bien Phu arm of the Paleotethys". Leloup et al. (1995) correlated the Dien Bien Suture with the Jinsha River Suture as fault markers of the Ailaoshan–Red River Fault, calculating that Indochina extruded ~500–700 km along the Ailaoshan left-lateral strike slip fault during 35–22 Ma. However, recent geochronological studies have disclosed that initiation of the Dien Bien Phu Fault occurred after 228 Ma (Lin et al., 2009; Roger et al., 2014); the Fault thus mismatches the volcanic arc I-type granites described in this paper. Furthermore, structural studies (DGM, 1991; Lepvrier et al., 1997; Lin et al., 2009; Faure et al., 2014; Roger et al., 2014) show that the Song Ma Suture is right-laterally offset ~30–40 km by the Dien Bien Phu Fault; the strata and fold axes have also bent eastward, but the primary structure of the Truong Son Belt has not been significantly altered. So, the Dien Bien Phu Fault does not present a suture branch separating the Qamdo–Simao Block from the Indochina Block. Thus, the Nan Suture should connect northward with the Jinghong Suture (Sone and Metcalfe, 2008; Faure et al., 2014), and the Qamdo–Simao–Indochina Block should be a united block (Fig. 11).

The similarity of the characteristics of the Qamdo–Simao and Indochina blocks when treated as a united block can be proven using other evidence. First, although Lepvrier et al. (1997, 2004) suggested that the Indochina Block subducted eastward under South China during the Late Permian–Early Triassic, increasing quantities of structural, geochronological and geochemical data confirm that the geometry of the block convergence between Indochina and South China suggests a westward subduction of South China under Indochina (Liu et al., 2012; Faure et al., 2014; this paper). The same is true for South China subducting westward under the Qamdo–Simao Block. The precise timing of the two block convergences has been corrected from 220 Ma (Rb–Sr age, Wang et al., 2000) to 270–240 Ma (Jian et al., 2008, 2009; Lai et al., 2014), almost the same age as that we obtained for this paper. Secondly, the 440–400 Ma granite complexes found along the Jinsha River Suture in China (e.g., Jian et al., 2009) have also been found along the Song Ma Suture (this paper) and along the Kontum Massif in Vietnam (e.g. Carter et al., 2001; Nagy et al., 2001; Sanematsu et al., 2011). There is no magmatic event either in the

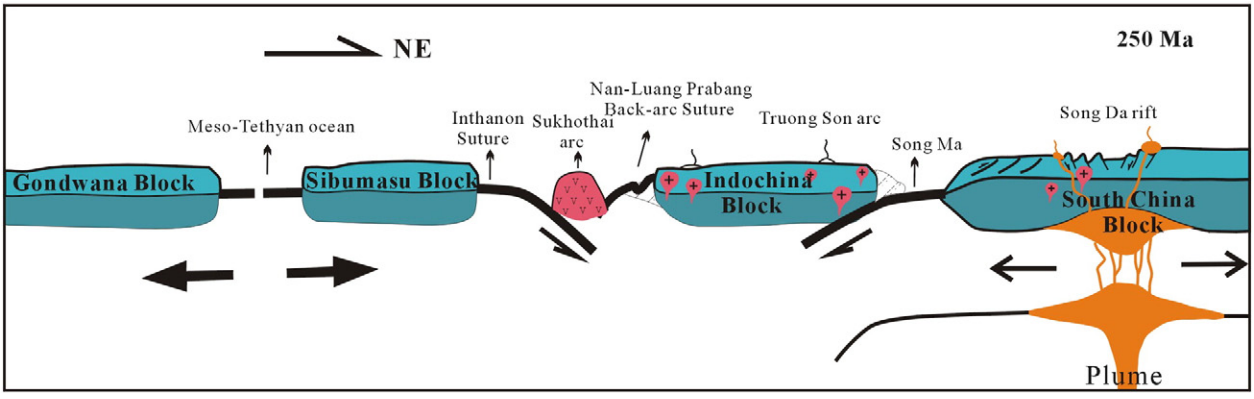

Fig. 12. Geodynamic model of the convergence of the Southeast Asian blocks during closure of the Paleotethyan Ocean (after Jian et al., 2009; Liu et al., 2012; Faure et al., 2014).

Qamdo–Simao Block or in the Indochina Block from 400 Ma to 280 Ma. Thus the Qamdo–Simao Block and the Indochina Block should have experienced similar magmatic events from the Early Paleozoic to the Early Mesozoic. Indeed, the early Paleozoic magmatic event prior to the Indosinian magmatic event recorded in the Sibumasu–Bao Shan–South Qiangtang Block occurred at ~500–470 Ma (e.g. Dong et al., 2013; Lin et al., 2013; Hu et al., 2015), ~100–60 Ma earlier than that in the Qamdo–Simao–Indochina Block. Further, evidence of the existence of the same Gigantopteris flora and warm-water fauna in the Indochina and Qamdo–Simao Blocks proves that they were once rifted and drifted northward from Gondwana in the Early Devonian (Metcalfe, 1996, 1999). Lastly, as deduced from εNd and T_{MD2} ages, the principal period of crust formation in the Qamdo–Simao Block was ~1.4–1.7 Ga (e.g. Zhai et al., 2012; Zhang et al., 2014), similar to that of the Indochina Block.

5.3. The Jinsha River Suture–Song Ma Suture–Kontum Massif as the boundary between the Qamdo–Simao–Indochina and South China blocks

The Late Permian–Early Triassic I-type granites detailed in this paper belong to the Truong Son Belt, thus corroborating the tectonic model of the South China Block subducting westward under the Indochina Block (Liu et al., 2012; Faure et al., 2014). In interpreting the relation between the Song Ma and Song Chay sutures in northern Vietnam, Faure et al. (2014) suggested that these two northern Vietnamese belts are parts of a single orogen dismembered by Cenozoic wrenching along the Red River Fault. There are several reasons for disagreeing with this hypothesis.

First, structural studies (Lepvrier et al., 1997, 2004, 2008; Tran et al., 2014) show an E–W strike, shifting to a N–S strike, along the Tam Ky–Phuoc Son Suture in the southern part of the Truong Son Belt, and north of the Kontum Massif. Southward, the Tam Ky–Phuoc Son Suture connects with the Poko Suture west of the Kontum Massif. Geochronological magmatism (e.g. Lan et al., 2000; Carter et al., 2001; Nagy et al., 2001; Owada et al., 2007; Sanematsu et al., 2011) and metamorphism (e.g. Osanai et al., 2001; Lan et al., 2003; Osanai et al., 2004; Nakano et al., 2007) relating to the Poko Suture also renders ages of between 260 Ma and 240 Ma. Lepvrier et al. (2008) even suggested that the Kontum Massif subducted westward under the Indochina Block, with the time and manner the same as for the two blocks along the Song Ma Suture (this paper; Liu et al., 2012; Faure et al., 2014). If the Song Ma Suture is therefore offset from the Jinsha–Song Chay Suture, the role of the Kontum Massif in the convergence of Indochina and South China vis-à-vis the Poko Suture becomes difficult to interpret.

Second, if the Song Ma Suture Zone is taken as forming the northern segment of the Song Chay Suture, there would be no system of tectonic units related to the Indochina orogenic zone around the Song Chay Suture. For example, no volcanic arc belt exists on either side of the Song Chay Suture; granites southwest of the Song Chay Suture are A-type granite with positive Nd(t) values (Pham et al., 2013), and are thus related to the Song Da Rift.

Third, in the Indochina Block, there is no other continental-scale ductile shear zone that, coupled with the Ailaoshan–Red River Fault, could produce the documented Early Miocene Truong Son Belt extrusion. For example, within the Indochina Block, the Dien Bien Phu Fault forms the western boundary of the Truong Son Belt, but geochronological and structural studies show that it was a right-lateral strike slip fault after 228 Ma, with an offset of ~30–40 km; the Fault, as the southernmost part of the Xianshuihe fault system, has been active from ~5 Ma to the present, with a left-lateral offset of <10 km (e.g. Wang et al., 1998; Zuchiewicz et al., 2004; Koszowska et al., 2007; Lin et al., 2009; Roger et al., 2014).

We therefore propose that the Jinsha River Suture, the Song Ma Suture and the Kontum Massif form the boundary between the Indochina and South China blocks.

5.4. The Emeishan Plume: the dynamics of a Permo-Triassic block convergence

Southeast Asia is a composite landmass of Gondwana-derived continental blocks. Having been detached from the northeastern margin of Gondwana, thes progressively assembled and accreted to form a proto-Asian continental plate. A major part of this evolution took place from the Mid Paleozoic to the Early Mesozoic. Several episodes of rifting and northward drifting occurred, followed by subduction and subsequent narrowing and closure of different branches of the Paleotethyan Ocean (e.g., Sengör, 1979; Sengor, 1984; Metcalfe, 1996; Hutchison, 1989; Lepvrier et al., 1997; Metcalfe, 1999, 2002; Lepvrier et al., 2004, 2008). Without doubt, the closure of the Paleotethyan Ocean and the opening of the Mesotethyan Ocean provided the main dynamics for the convergence of the Sibumasu, Qamdo–Simao–Indochina and South China blocks. Against this background, we would also suggest that the Emeishan Plume contributed to the convergence of the Qamdo–Simao–Indochina and South China blocks.

The Emeishan basalts, also known as the Emeishan large igneous province (ELIP), outcrop principally in the Chinese provinces of Sichuan, Yunnan and Guizhou, as well as the Song Da region of northern Vietnam. The ELIP is composed mainly of flood basalts and mafic–ultramafic intrusions. The volcanic sequence ranges in thickness from several hundred meters in the east to nearly 5 km in the west (Chung and Jahn, 1995; Song et al., 2001; Xu et al., 2001; Xiao et al., 2004). The lavas include picrites, tholeiites and basaltic andesites, all of which are believed to have formed from an upwelling mantle plume (Chung and Jahn, 1995; Xu et al., 2001; Zhou et al., 2006). Recent research has found that Late Permian A-type granite is related to the Emeishan Plume in the Panzhihua and Dali rifts in the Sichuan–Yunnan area (Shellnutt and Zhou, 2007; Shellnutt et al., 2009), similar to a study of the Song Da Rift (Pham et al., 2013). Permian flood basalts and associated mafic–ultramafic intrusions form a narrow (≤20 km), NW-trending belt >350 km long in the Jinping–Song Da Rift. The belt is bounded by the Ailaoshan–Red River Fault Zone to the northeast and the Jinsha–Song Ma Suture to the southwest (Wang et al., 2007). South of this, there is no report of Emeishan basalts outcropping in the Kontum Massif, but a NW–SE striking normal shear zone has developed in the Ngoc Linh and Kannack complexes, which is composed of HT to UHT metamorphic rocks (Osanai et al., 2004; Lepvrier et al., 2008). Both the Ngoc Linh and the Kannak complexes are locally intruded by granitic rocks, with fine-grained gabbro enclaves; the igneous activity and HT to UHT metamorphism coincide with each other at 260 Ma to 250 Ma. An upwelling mantle plume would explain the formation of syntectonic magmatism and HT–UHT metamorphism (Osanai et al., 2001, 2004; Owada et al., 2007). The plume related to the Emeishan Plume thus appears to represent a particular tectonic feature at the western boundary of the South China Block.

I-type volcanic arc granites in the Late Permian–Early Triassic can be treated as an index of the subduction between the Sibumasu, Indochina and South China blocks during the closure of the Paleotethyan Ocean (Carter et al., 2001; Lepvrier et al., 2004, 2008; Liu et al., 2012). Subsequently, S-type granites with ages of 220 Ma to 200 Ma, as well as I-type granites of Late Mesozoic age, developed at the western boundary of the Sibumasu Block (e.g., Charusiri et al., 1993; Searle et al., 2012), indicating compressional conditions during the Mesozoic. In contrast, A-type granites developed after 200 Ma in the South China Block. It has been suggested that these magmas were generated as a consequence of intraplate extension in the western part of the South China Block (e.g. Chung et al., 1997; Lan et al., 2000; Maluski et al., 2001). The different stresses prevalent in the South China Block vis-à-vis the Sibumasu Block could be attributed to the dynamic conditions produced by the Emeishan Plume in the mantle after 260 Ma. We therefore propose that the Emeishan Plume formed part of the dynamic driving Permo-Triassic block convergence and subsequent extension into the South China Block (Fig. 12).

6. Conclusions

33 samples from six granite complexes along the road from Phonsavan to Sam Neua in northern Laos were selected for zircon U–Pb age, Lu–Hf ratio and whole-rock major, trace and rare earth element analyses. Geochronological and geochemical data from these samples can be summarized as follows:

1) The zircon U–Pb ages of 600 spots from 16 samples taken from five granite complexes range from 256 Ma to 234 Ma. 256–234 Ma magmatic arc granites mismatch the initiation time of the Dien Bien Phu Fault. The existence of the Dien Bien Phu Suture can therefore be repudiated. This evidence further suggests the existence of a united Qamdo–Simao–Indochina Block.
2) The εHf(t) values of zircon Lu–Hf data from a total of 201 spots from 20 samples are generally negative, with corresponding T_{DM2} ages dated to the Late Paleoproterozoic. Zircon inheritance ages and T_{MD2} ages suggest that the formation of the main crust of the Indochina Block was during the Late Paleoproterozoic; these ages are much younger than the Archean ages obtained in the Cavinh Complex of northern Vietnam, east of the Song Ma Suture. Thus, the different crustal evolutions of the Indochina Block and the block east of the Song Ma Suture further confirm that the boundary between Indochina and South China is the Song Ma Suture, rather than the Song Da or Song Chay sutures.
3) Major, trace and rare earth element data from the granitic rocks of five complexes indicate the presence of mainly peraluminous high-K calcalkaline granite. The Indochina granite samples have similar patterns in their chondrite and primitive mantle normalized REE and trace element plots, marked by variable enrichments in Rb, Ba, Th and Ce, and depletions in Ta, Nb, Sr and Ti, all typical of I-type volcanic arc granites. These granites, together with other tectonic units of the Song Ma Suture, suggest a westward subduction of the South China Block beneath the Qamdo–Simao–Indochina Block.
4) 440–404 Ma and 256–234 Ma I-type granites suggest that the boundary between Indochina and South China should be the Jinsha River Suture–Song Ma Suture–Kontum Massif, rather than the Jinsha–Song Chay Suture.
5) Both the Emeishan basalt and granite complexes form part of the tectonic units of the South China Block subducting westward under the Qamdo–Simao–Indochina Block. The plume beneath the Emeishan basalt has also contributed to the convergence of the two blocks, following the opening of the Mesotethyan Ocean.

Supplementary data to this article can be found online at http://dx.doi.org/10.1016/j.gr.2015.11.011.

Acknowledgments

This research was funded jointly by the Basic Science Research Fund of the Institute of Geomechanics, CAGS (grant nos. DZLXJK201410, DZLXJK201406); the China Geological Survey (grant nos. 12120115000701, 12120114002101); and the National Natural Science Foundation of China (grant no. 41172192). We would like to thank Professors Ian Metcalfe, Chris Morley, Sunlin Chung and two anonymous reviewers for their constructive advice, which has greatly improved the quality of the draft. Thanks are also due to Doctors Yunpeng Dong and Sanghoon Kwon for their work on the manuscript.

References

Barr, S.M., MacDonald, A.S., 1987. Nan River suture zone, northern Thailand. Geology 15, 907–910.

Barr, S.M., MacDonald, A.S., Dunning, G.R., Ounchanum, P., Yaowanoiyothin, W., 2000. Petrochemistry, U–Pb (zircon) age, and palaeotectonic setting of the Lampang volcanic belt, northern Thailand. Journal of the Geological Society of London 157, 553–563.

Beckinsale, R.D., Suensilpong, S., Nakapadungrat, S., 1979. Geochronology and geochemistry of granite magmatism in Thailand in relation to plate tectonic models. Journal of the Geological Society of London 136, 529–540.

Blichert-Toft, J., Albarède, F., 1997. The Lu–Hf geochemistry of chondrites and the evolution of the mantle–crust system. Earth and Planetary Science Letters 148, 243–258.

Boynton, W.V., 1984. Cosmochemistry of the Rare Earth Elements: Meteorite Studies. Elsevier Science Publishing Company, Amsterdam.

Burrett, C., Zaw, K., Meffre, S., Lai, C.K., Khositanont, S., Chaodumrong, P., Udchachon, M., Ekins, S., Halpin, J., 2014. The configuration of Greater Gondwana: evidence from LA ICPMS, U–Pb geochronology of detrital zircons from the Palaeozoic and Mesozoic of Southeast Asia and China. Gondwana Research 26 (1), 31–51.

Carter, A., Clift, P.D., 2008. Was the Indosinian orogeny a Triassic mountain building or a thermotectonic reactivation event? Comptes Rendus Geoscience 340, 83–93.

Carter, A., Roques, D., Bristow, C., Kinny, P., 2001. Understanding Mesozoic accretion in Southeast Asia: significance of Triassic thermotectonism (Indochina Orogeny) in Vietnam. Geology 29 (3), 211–214.

Chappell, B.W., White, A.J.R., 1992. I- and S-type granites in the Lachlan Fold Belt. Transactions of the Royal Society of Edinburgh: Earth Sciences 83 (1–2), 1–26.

Charusiri, P., Clark, A.H., Farrar, E., Archibald, D., Charusiri, B., 1993. Granites belts in Thailand: evidence from the $^{40}Ar/^{39}Ar$ geochronological and geological syntheses. Journal of Southeast Asian Earth Sciences 8, 127–136.

Chung, S.L., Jahn, B.M., 1995. Plume–lithosphere interaction in generation of the Emeishan flood basalts at the Permian–Triassic boundary. Geology 23, 889–892.

Chung, S., Lee, T., Lo, C., Wang, P., Chen, C., Yem, N., Tran, T.H., Wu, G., 1997. Intraplate extension prior to continental extrusion along the Ailao Shan–Red River shear zone. Geology 25 (4), 311–314.

Department of Geological and Minerals of Vietnam (DGMV), 2005. Geology and Mineral Resources Map of Phong Saly–Dien Bien Phu Sheet, Scale 1:200000, With the Explanatory Note, Hanoi.

Department of Geology and Mining, Lao P.D.R. (DGM), 1991. Geological and mineral occurrence map. 1:1000000 scale. British Geological Survey and Department of Geology and Mines.

Dong, M., Dong, G., Mo, X., Santosh, M., Zhu, D., Yu, J., Nie, F., Hu, Z., 2013. Geochemistry, zircon U–Pb geochronology and Hf isotopes of granites in the Baoshan Block, Western Yunnan: implications for Early Paleozoic evolution along the Gondwana margin. Lithos 179, 36–47.

Faure, M., Lepvrier, C., Nguyen, V., Vu, T., Lin, W., Chen, Z., 2014. The South China block–Indochina collision: where, when, and how? Journal of Southeast Asian Earth Sciences 79, 260–274.

Ferrari, O.M., Hochard, C., Stampfli, G.M., 2008. An alternative plate tectonic model for the Palaeozoic–Early Mesozoic Palaeotethyan evolution of Southeast Asia (Northern Thailand–Burma). Tectonophysics 451, 346–365.

Griffin, W.L., Wang, X., Jackson, S.E., Pearson, N.J., O'Reilly, S.Y., Xu, X., Zhou, X., 2002. Zircon chemistry and magmamixing, SE China: *in-situ* analysis of Hf isotopes, Tonglu and Pingtan igneous complexes. Lithos 61, 237–269.

Harris, N.B.W., Pearce, J.A., Tindle, A.G., 1986. Geochemical characteristics of collision-zone magmatism. In: Coward, M.P., Rles, A.C. (Eds.), Collision Tectonics. Geological Society, London, Special Publications vol. 19, pp. 67–81.

Hu, P., Zhai, Q., Jahn, B., Wang, J., Lee, H., Tang, S., 2015. Early Ordovician granites from the South Qiangtang terrane, northern Tibet: implications for the early Paleozoic tectonic evolution along the Gondwanan proto-Tethyan margin. Lithos. http://dx.doi.org/10.1016/j.lithos.2014.12.020.

Hutchison, C.S., 1989. South-East Asian oil, gas, coal and mineral deposits. Oxford Monographs on Geology and Geophysics, p. 13.

Jackson, S.E., Pearson, N.J., Griffin, W.L., Belousova, E.A., 2004. The application of laser ablation-inductively coupled plasma-mass spectrometry to in situ U–Pb zircon geochronology. Chemical Geology 211 (1–2), 47–69.

Janvier, P., Tong-Dzuy, T., Ta Hoa, P., Doan Nhat, T., 1997. The Devonian vertebrates (Placodermi, Sarcopterygii) from Central Vietnam and their bearing on the Devonian paleogeography of Southeast Asia. Journal of Asian Earth Sciences 15, 393–406.

Jian, P., Liu, D.Y., Sun, X.M., 2008. SHRIMP dating of the Permo-Carboniferous Jinshajiang ophiolite, southwestern China: geochronological constraints for the evolution of Paleo-Tethys. Journal of Asian Earth Sciences 32, 371–384.

Jian, P., Liu, D.Y., Kröner, A., Zhang, Q., Wang, Y.Z., Sun, X.M., Zhang, W., 2009. Devonian to Permian plate tectonic cycle of the Paleo-Tethys Orogen in southwest China (II): insights from zircon ages of ophiolites, arc/back-arc assemblages and withinplate igneous rocks and generation of the Emeishan CFB province. Lithos 113, 767–784.

Koszowska, E., Wolska, A., Zuchiewicz, W., Nguyen, Q., Pecskay, Z., 2007. Crustal contamination of Late Neogene basalts in the Dien Bien Phu Basin, NW Vietnam: some insights from petrological and geochronological studies. Journal of Asian Earth Sciences 29, 1–17.

Lai, C.K., Meffre, S., Crawford, A.J., Khin, Z., Xue, C.D., Halpin, J., 2014. The Western Ailaoshan volcanic belts and their SE Asia connection: a new tectonic model for the Eastern Indochina Block. Gondwana Research 26 (1), 52–74.

Lan, C.Y., Chung, S.L., Shen, J.J., Lo, C.H., Wang, P.L., Tran, T.H., Thanh, H.H., Mertzman, S.A., 2000. Geochemical and Sr–Nd isotopic characteristics of granitic rocks from northern Vietnam. Journal of Asian Earth Sciences 267–280.

Lan, C.Y., Chung, S.L., Lo, C.H., Lee, T.Y., Wang, P.L., Li, H., Toan, D.V., 2001. First evidence for Archean continental crust in northern Vietnam and its implications for crustal and tectonic evolution in Southeast Asia. Geology 29 (3), 219–222.

Lan, C., Chung, S., Trinh, V.L., Lo, C., Lee, T., Mertzman, S., Shen, J., 2003. Geochemical and Sr–Nd isotopic constraints from the Kontum massif, central Vietnam on the crustal evolution of the Indochina block. Precambrian Research 122, 7–27.

Leloup, P.H., Lacassin, R., Tapponnier, R., Zhong, D., Lui, X., Zhang, L., Ji, S., Trinh, P.T., 1995. The Ailao Shan–Red River shear zone (Yunnan, China), Tertiary transform boundary of Indochina. Tectonophysics 251, 3–84.

Lepvrier, C., Maluski, H., Nyugen, V.V., Roques, D., Axente, V., Rangin, G., 1997. Indochina NW-trending shear zones within the Truong Son belt (Vietnam). Tectonophysics 283, 105–127.
Lepvrier, C., Maluski, H., Tich, V.V., Leyreloup, A., Truong, T.P., Nyugen, V.V., 2004. The Early Triassic Indochina orogeny in Vietnam (Truong Son Belt and Kontum Massif): implications for the geodynamic evolution of Indochina. Tectonophysics 393, 87–118.
Lepvrier, C., Nyugen, V.V., Maluski, H., Thi, P.T., Tich, V.V., 2008. Indosinian tectonics in Vietnam. Comptes Rendus Geoscience 340, 94–111.
Lepvrier, C., Faure, M., Nyugen, V.V., Tich, V.V., Lin, W., Thang, T.T., Phuong, T.H., 2011. North-directed Triassic nappes in Northeastern Vietnam (East Bac Bo). Journal of Asian Earth Sciences 41, 56–68.
Liew, T.C., McCulloch, M.T., 1985. Genesis of granitoid batholiths of Peninsular Malaysia and implications for models of crustal evolution: evidence from Nd–Sr isotopic and U–Pb zircon study. Geochimica et Cosmochimica Acta 49, 587–600.
Lin, T., Lo, C., Chung, S., Wang, P., Yeh, M., Lee, T., Lan, C., Nyugen, V.V., Tran, T., 2009. Jurassic dextral movement along the Dien Bien Phu Fault, NW Vietnam: constraints from $^{40}Ar/^{39}Ar$ geochronology. The Journal of Geology 117, 192–199.
Lin, Y., Yeh, M., Lee, T., Chung, S., Lizuka, Y., Charusiri, P., 2013. First evidence of the Cambrian basement in Upper Peninsula of Thailand and its implication for crustal and tectonic evolution of the Sibumasu terrane. Gondwana Research 24, 1031–1037.
Liu, Y.S., Hu, Z.C., Gao, S., Günther, D., Xu, J., Gao, C.G., Chen, H.H., 2008. In situ analysis of major and trace elements of anhydrous minerals by LA-ICP-MS without applying an internal standard. Chemical Geology 257, 34–43.
Liu, J., Tran, M., Tang, Y., Nguyen, Q.L., Tran, T.H., Wu, W., Chen, J., Zhang, Z., Zhao, Z., 2012. Permo-Triassic granitoids in the northern part of the Truong Son belt, NW Vietnam: geochronology, geochemistry and tectonic implications. Gondwana Research 122, 628–644.
Ludwig, K.R., 2003. User's manual for Isoplot 3.00: a geochronological toolkit for Microsoft Excel. Berkeley Geochronology Center Special Publication 4.
Maluski, H., Lepvrier, C., Jolivet, L., Carter, A., Roques, D., Beyssac, O., Nguyen, D.T., Ta, T.T., Avigad, D., 2001. Ar–Ar and fission track ages in the Song Chay massif: early Triassic and Cenozoic tectonics in northern Vietnam. Journal of Asian Earth Sciences 19, 233–248.
Maniar, P.D., Piccoli, P.M., 1989. Tectonic discrimination of granitoids. Geological Society of America Bulletin 101, 635–643.
Metcalfe, I., 1996. Pre-Cretaceous evolution of SE Asian terranes. In: Hall, R., Blundell, D. (Eds.), Tectonic evolution of Southeast Asia. Geological Society of London Special Publication 106, pp. 97–122.
Metcalfe, I., 1999. Gondwana dispersion and Asian accretion: an overview. In: Metcalfe, I. (Ed.), Gondwana dispersion and Asian accretionFinal Results Volume for IGCP Project 321. Balkema, Rotterdam, pp. 9–28.
Metcalfe, I., 2002. Permian tectonic framework and paleogeography of SE Asia. Journal of Asian Earth Sciences 20, 551–566.
Metcalfe, I., 2006. Palaeozoic and Mesozoic tectonic evolution and palaeogeography of East Asian crustal fragments: The Korean Peninsula in context. Gondwana Research 9, 24–46.
Metcalfe, I., 2013. Gondwana dispersion and Asian accretion: tectonic and palaeogeographic evolution of the eastern Tethys. Journal of Asian Earth Sciences 66, 1–33.
Middlemost, E.A.K., 1985. Magmas and Magmatic Rocks. Longman, London, pp. 1–266.
Nagy, E.A., Maluski, H., Lepvrier, Q., Scharer, U., Thi, P.T., Leyreloup, A., 2001. Geodynamic significance of the Kontum massif in Central Vietnam: composite $^{40}Ar/^{39}Ar$ and U/Pb ages from Paleozoic to Triassic. Journal of Geology 109, 755–770.
Nakano, N., Osanai, Y., Owada, N., Hayasaka, Y., Tran, N.N., 2007. Permo-Triassic Barrovian metamorphism in the Kontum massif, central Vietnam: constraints on continental collision tectonics in Southeast Asia. Gondwana Research 12, 438–453.
Osanai, Y., Owada, M., Tsunogae, T., Toyoshima, T., Hokada, T., Long, T.V., Sajeev, K., Nakano, N., 2001. Ultrahigh-temperature politic granulites from Kontum massif, central Vietnam: evidence for East Asia juxtaposition at ca. 250 Ma. Gondwana Research 4, 720–723.
Osanai, Y., Nakano, N., Owada, M., Tran, N.N., Toyoshima, T., Tsunogae, T., Pham, B., 2004. Permo-Triassic ultrahigh-temperature metamorphism in the Kontum massif, central Vietnam. Journal of Mineralogical and Petrological Sciences 106, 13–25.
Owada, M., Osanai, Y., Nakano, N., Tran, N.N., Binh, P., Tsunogae, T., Toyoshima, T., Kagami, H., 2007. Crustal anatexis and formation of two types of granitic magmas in the Kontum massif, Central Vietnam: implications for magma processes in collision zone. Gondwana Research 12, 428–437.
Peccerillo, R., Taylor, S.R., 1976. Geochmistry of Eocene calc-alkaline volcanic rocks from the Kastamonu area, Northern Turkey. Contributions to Mineralogy and Petrology 58, 63–81.
Pham, T.H., Chen, F.K., Nguyen, T.B., Nguyen, Q.C., Li, S.H., 2013. Geochemistry and zircon U–Pb ages and Hf isotopic composition of Permian alkali granitoids of the Phan Si Pan zone in northwest Vietnam. Journal of Geodynamics 69, 106–121.
Qian, X., Feng, Q., Wang, Y., Chonglakmani, C., Monjai, D., 2015. Geochronological and geochemical constraints on the mafic rocks along the Luang Prabang zone: Carboniferous back-arc setting in northwest Laos. Lithos. http://dx.doi.org/10.1016/j.lithos. 2015.07.019.
Racheboeuf, P., Janvier, P., Ta Hoa, P., Vannier, J., Wang, S.Q., 2005. Lower Devonian vertebrates, arthropods and brachiopods from northern Vietnam. Geobios 38, 533–551.
Racheboeuf, P., Ta Hoa, P., Nguyen, H.H., Feist, M., Janvier, P., 2006. Brachiopods, crustaceans, vertebrates, and charophytes from the Devonian Ly Hoa, Nam Can and Dong Tho formations of Central Vietnam. Geodiversitas 28, 5–36.
Roger, F., Jolivet, M., Maluski, H., Respaut, J., Müncha, P., Paquette, J., Vu Vand, T., Nguyen, V.V., 2014. Emplacement and cooling of the Dien Bien Phu granitic complex: implications for the tectonic evolution of the Dien Bien Phu Fault (Truong Son Belt, NW Vietnam). Gondwana Research 26, 785–801.
Sanematsu, K., Murakam, H., Duangsurigna, S., Vilayhack, S., Duncan, R., Watanabe, Y., 2011. $^{40}Ar/^{39}Ar$ ages of granitoids from the Truong Son fold belt and Kontum massif in Laos. Journal of Mineralogical and Petrological Sciences 106, 13–25.
Searle, M.P., Whitehouse, M.J., Robb, J., Ghani, A.A., Hutchison, C.S., Sone, M., Ngi, S.W., Roseiee, M.H., Chung, S.L., Oliver, G.J.H., 2012. Tectonic evolution of the Sibumasu–Indochina terrane collision zone in Thailand and Malaysia: constraints from new U–Pb zircon chronology of SE Asian tin granitoids. Journal of the Geological Society, London 169, 489–500.
Sengör, A.M.C., 1979. Mid-Mesozoic closure of Permo-Triassic Tethys and its implications. Nature 279, 590–593.
Sengor, A.M.C., 1984. The Cimmeride orogenic system and the tectonics of Eurasia. Geological Society of America Special Papers 195, 1–74.
Shellnutt, J.G., Zhou, M.F., 2007. Permian peralkaline, peraluminous and metaluminous A-type granites in the Panxi district, SW China: their relationship to the Emeishan mantle plume. Chemical Geology 243, 286–316.
Shellnutt, J.G., Zhou, M.F., Zellmer, G., 2009. The role of Fe–Ti oxide crystallization in the formation of A-type granitoids with implications for the Daly gap: an example from the Permian Baima Igneous Complex. Chemical Geology 259, 204–217.
Singharajwarapan, S., Berry, R., 2000. Tectonic implications of the Nan Suture Zone and its relationship to the Sukhothai Fold Belt, Northern Thailand. Journal of Asian Earth Sciences 18, 663–673.
Sone, M., Metcalfe, I., 2008. Parallel Tethyan suture in mainland Southeast Asia: new insights from Paleo-Tethys closure and implications for the Indosinian orogeny. Comptes Rendus Geoscience 340, 166–179.
Song, X.Y., Zhou, M.F., Hou, Z.Q., Cao, Z.M., Wang, Y., Li, Y., 2001. Geochemical constraints on the mantle source of the Upper Permian Emeishan continental flood basalts, southwestern China. International Geology Review 43, 213–225.
Streckeisen, A., 1967. Classification and nomenclature of igneous rocks. Final report of an inquiry. Neues Jahrbuch für Mineralogie Abhandlungen 107, 144–204.
Sun, S.S., McDonough, W.F., 1989. Chemical and isotopic systematics of oceanic basalts: implications for mantle composition and processes. In: A.D., Saunders, M.J., Norry (Eds.), Magmatism in the ocean basins. Geological Society, London, Special Publications 42, pp. 313–345.
Tran, H.T., Khin, Z., Halpin, J., Manaka, T., Meffre, S., Lai, C.K., Lee, Y.J., Le, V.H., Dinh, S., 2014. The Tam Ky–Phuoc Son Shear Zone in Central Vietnam: tectonic andmetallogenic implications. Gondwana Research 26 (1), 144–164.
Ueno, K., 2003. The Permian fusulinoidean faunas of the Sibumasu and Baoshan blocks: their implications for the paleogeographic and paleoclimatologic reconstruction of the Cimmerian continent. Palaeogeography, Palaeoclimatology, Palaeoecology 193, 1–24.
Wang, E., Burchfiel, B.C., Royden, L.H., Chen, L., Chen, J., Li, W., Chen, Z., 1998. Late Cenozoic Xianshuihe–Xiaojiang, Red River, and Dali fault systems of southwestern Sichuan and central Yunnan, China. Geological Society of America Special Papers 327, 1–108.
Wang, X., Metcalfe, I., Jian, P., He, L., Wang, C., 2000. The Jinshajiang–Ailaoshan Suture Zone, China: tectonostratigraphy, age and evolution. Journal of Asian Earth Sciences 18 (6), 675–690.
Wang, C.Y., Zhou, M.F., Qi, L., 2007. Permian flood basalts and mafic intrusions in the Jinping (SW China)–Song Da (northern Vietnam) district: mantle sources, crustal contamination and sulfide segregation. Chemical Geology 243, 317–343.
Whalen, J.B., Currle, K.L., Chappell, B.W., 1987. A-type granites: geochemical characteristics, discrimination and petrogenesis. Contributions to Mineralogy and Petrology 95, 407–419.
Wu, H., Boulter, C.A., Ke, B., Stow, D.A.V., Wang, Z., 1995. The Changning–Menglian suture zone; a segment of the major Cathaysian–Gondwana divide in Southeast Asia. Tectonophysics 242, 267–280.
Wu, F.Y., Yang, Y.H., Xie, L.W., Yang, J.H., Xu, P., 2006. Hf isotopic compositions of the standard zircons and baddeleyites used in U–Pb geochronology. Chemical Geology 234, 105–126.
Xiao, L., Xu, Y.G., Mei, H.J., Zheng, Y.F., He, B., Pirajno, F., 2004. Distinct mantle sources of low-Ti and high-Ti basalts from the western Emeishan large igneous province, SW China: implications for plume–lithosphere interaction. Earth and Planetary Science Letters 228, 525–546.
Xie, L.W., Zhang, Y.B., Zhang, H.H., Sun, J.F., Wu, F.Y., 2008. *In situ* simultaneous determination of trace elements, U–Pb and Lu–Hf isotopes in zircon and baddeleyite. Chinese Science Bulletin 53, 1565–1573.
Xu, Y., Chung, S.L., Jahn, B.M., Wu, G., 2001. Petrologic and geochemical constraints on N the petrogenesis of Permian–Triassic Emeishan flood basalts in southwestern China. Lithos 58, 145–168.
Zhai, Q., Jahn, B., Su, L., Wang, J., Mo, X., Lee, H., Wang, K., Tang, S., 2012. Triassic arcmagmatismin the Qiangtang area, northern Tibet: zircon U–Pb ages, geochemical and Sr–Nd–Hf isotopic characteristics, and tectonic implications. Journal of Asian Earth Sciences 63, 162–178.
Zhang, L., Ding, L., Pullen, A., Xu, Q., Liu, D., Cai, F., Yue, Y., Lai, Q., Shi, R., Ducea, M., Kapp, P., Chapman, A., 2014. Age and geochemistry of western Hoh–Xil–Songpan–Ganzi granitoids, northern Tibet: implications for the Mesozoic closure of the Paleo-Tethys Ocean. Lithos 190–191, 328–348.
Zhou, M.F., Zhao, J.H., Qi, L., Su, W.C., Hu, R.Z., 2006. Zircon U–Pb geochronology and elemental and Sr–Nd isotope geochemistry of Permian mafic rocks in the Funing area, SW China. Contributions to Mineralogy and Petrology 151, 1–19.
Zuchiewicz, W., Cuong, N.Q., Bluszcz, A., Michalik, M., 2004. Quaternary sediments in the Dien Bien Phu fault zone, NW Vietnam: a record of young tectonic processes in the light of OSL-SAR dating results. Geomorphology 60, 269–302.